

## Article

# The Influence of Track Structure Parameters on the Dynamic Response Sensitivity of Heavy Haul Train-LVT System

Zhi-Ping Zeng<sup>1,2</sup>, Yan-Cai Xiao<sup>1</sup>, Wei-Dong Wang<sup>1,2,\*</sup>, Xu-Dong Huang<sup>1</sup>, Xiang-Gang Du<sup>3</sup>, Lan-Li Liu<sup>4</sup>, Joseph Elejo Victor<sup>1,5</sup>, Zhong-Lin Xie<sup>1</sup>, Yu Yuan<sup>6</sup> and Jun-Dong Wang<sup>1</sup>

<sup>1</sup> School of Civil Engineering, Central South University, Changsha 410075, China; 203160@csu.edu.cn (Z.-P.Z.); 214812219@csu.edu.cn (Y.-C.X.); samhuang@csu.edu.cn (X.-D.H.); joseph\_victor@yeah.net (J.E.V.); 8210202322@csu.edu.cn (Z.-L.X.); 174812173@csu.edu.cn (J.-D.W.)

<sup>2</sup> MOE Key Laboratory of Engineering Structures of Heavy Haul Railway, Central South University, Changsha 410075, China

<sup>3</sup> State Key Laboratory of High Speed Railway Track Technology, Beijing 100081, China; 16231169@bjtu.edu.cn

<sup>4</sup> China Railway Fifth Survey and Design Institute Group Co., Ltd., Beijing 102600, China; 174812176@csu.edu.cn

<sup>5</sup> Department of Civil Engineering, Faculty of Engineering, Ahmadu Bello University, Zaria 800242, Nigeria

<sup>6</sup> Information Engineering School, Nanchang University, Nanchang 330031, China; yuyuan@email.ncu.edu.cn

\* Correspondence: wd1997@csu.edu.cn



check for updates

**Citation:** Zeng, Z.-P.; Xiao, Y.-C.; Wang, W.-D.; Huang, X.-D.; Du, X.-G.; Liu, L.-L.; Victor, J.E.; Xie, Z.-L.; Yuan, Y.; Wang, J.-D. The Influence of Track Structure Parameters on the Dynamic Response Sensitivity of Heavy Haul Train-LVT System. *Appl. Sci.* **2021**, *11*, 11830. <https://doi.org/10.3390/app112411830>

Academic Editors: Araliya Mosleh, José A.F.O. Correia, Diogo Ribeiro and Anna M. Rakoczy

Received: 13 October 2021

Accepted: 2 December 2021

Published: 13 December 2021

**Publisher's Note:** MDPI stays neutral with regard to jurisdictional claims in published maps and institutional affiliations.



**Copyright:** © 2021 by the authors. Licensee MDPI, Basel, Switzerland. This article is an open access article distributed under the terms and conditions of the Creative Commons Attribution (CC BY) license (<https://creativecommons.org/licenses/by/4.0/>).

**Abstract:** **Background:** In order to study the applicability of Low Vibration Track (LVT) in heavy-haul railway tunnels, this paper carried out research on the dynamic effects of LVT heavy-haul railway wheels and rails and provided a technical reference for the structural design of heavy-haul railway track structures. **Methods:** Based on system dynamics response sensitivity and vehicle-track coupling dynamics, the stability of the upper heavy-haul train, the track deformation tendency, and the dynamic response sensitivity of the vehicle-track system under the influence of random track irregularity and different track structure parameters were calculated, compared and analyzed. **Results:** Larger under-rail lateral and vertical structural stiffness can reduce the dynamic response of the rail system. The vertical and lateral stiffness under the block should be set within a reasonable range to achieve the purpose of reducing the dynamic response of the system, and beyond a certain range, the dynamic response of the rail system will increase significantly, which will affect the safety and stability of train operation. **Conclusions:** Considering the changes of track vehicle body stability coefficients, the change of deformation control coefficients, and the sensitivity indexes of dynamic performance coefficients to track structure stiffness change, the recommended values of the vertical stiffness under rail, the lateral stiffness under rail, the vertical stiffness under block, and the lateral stiffness under block are, respectively 160 kN/mm, 200 kN/mm, 100 kN/mm, and 200 kN/mm.

**Keywords:** track structure parameters; heavy-haul railway; low vibration track; vehicle-track coupled system; dynamic response sensitivity

## 1. Introduction

Since the emergence of heavy-haul railway transportation in the middle of the 20th century, it has been widely valued by railways around the world, and has developed rapidly due to its large capacity, high efficiency, and low cost [1–3]. Traditional ballasted track structures have gradually been unable to meet the functional needs of heavy-haul railways in special sections, such as long tunnel segments, as Chinese standards for heavy-haul railway transit efficiency have improved. Therefore, the research and application of a new-type of ballastless track structure for heavy-haul railways has gradually become a major development direction of Chinese railways [4,5]. Simultaneously, as Chinese railway construction progresses, mainline railway will be capable of carrying trains traveling at speeds higher than 200 km/h, and more and more long tunnels are advised to apply ballastless tracks [6].

Ballasted tracks are commonly used in the subgrade section of heavy-haul railways, but the tunnel section is affected by the limitation of section clearance and the inconvenience of maintenance [7,8]. The transportation of coal and other materials frequently requires passing through long tunnels, the “Guiding Opinions on Optimization of Railway Engineering Design Measures” [9] proposed that for the tunnels exceeding 1 km, the section of the tunnel group should adopt the ballastless track structure, in order to ensure the clearance and ventilation in the tunnel, as well as the long-term stability of the track structure. In this context, low vibration track (LVT) has gradually gained attention in the selection of ballastless tracks in heavy-haul railway tunnels due to its excellent damping performance [10,11], as shown in Figure 1. Since LVT has a double-layer damping structure, consisting of under-rail rubber pads and under-block rubber pads, compared with other types of track structures, it can greatly reduce the impact of heavy-haul trains. Therefore, the LVT is to be applied in the Xikang railway, Qinling railway tunnel, Yiwang railway, Xiangyu railway and other long railway tunnels in China [12].

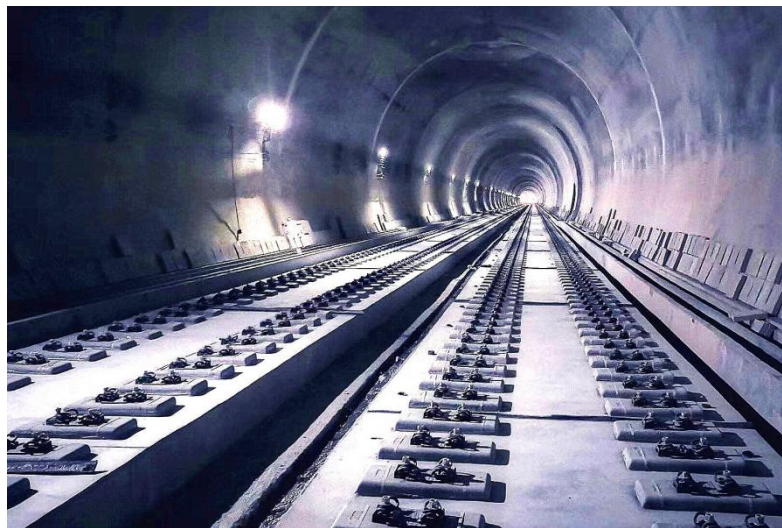
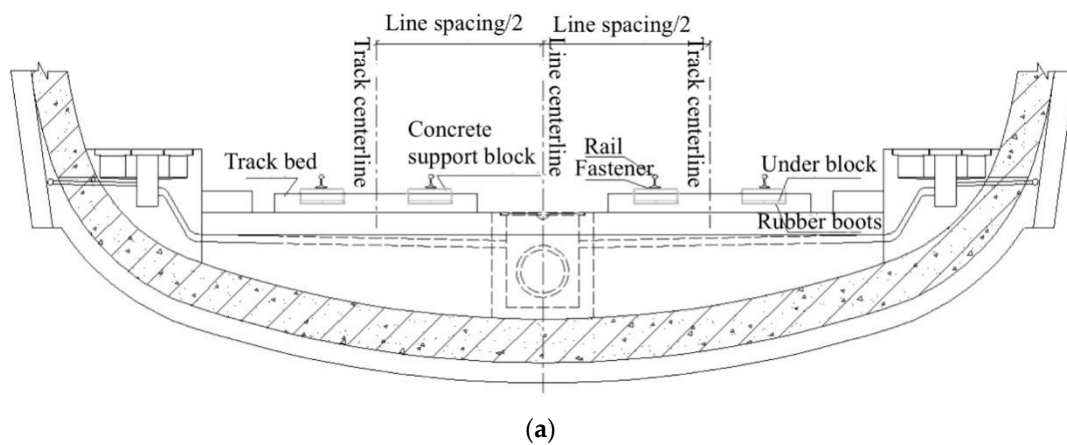


**Figure 1.** Heavy-haul train and LVT scene in the tunnel. (a) Design diagram of LVT section in tunnel and (b) LVT construction scene in the tunnel.

LVT was first tested in the Swiss National Railway Tunnel in 1966 and since then, Denmark, Britain, France, Portugal, and other countries have successively laid this kind of track. There are also many kinds of LVT in Chinese subway tunnels and long tunnels, such as the Qinling Tunnel, Wushaoling Tunnel, and Yindongpo Tunnel. LVT has good elasticity, but the supporting blocks are independent of each other, which may cause a bad dynamic between the wheel and rail and risk rail displacement under heavy loads if the

train is larger [13]. If the track stiffness is too low, it may cause the track dynamic geometric deviation to exceed the limit under high-speed running conditions, which will affect the safety and comfort of running [14,15]. Therefore, LVT is limited to railways operating at speeds below 200 km/h, and in China it is limited to railways operating at a speed of 120 km/h.

In order to conduct research on the application of LVT in heavy-haul railways, it is necessary to consider the basic parameters of the under-rail and under block that affect the dynamic characteristics of the vehicle-track vibration system. The changes in the stiffness of the fasteners, the stiffness of the track bed, and the sleeper spacing directly affect the vibration of the system, and different parameters have different effects on the vibration of the system [16]. Therefore, the analysis of the basic parameters under the track is of great significance to improve the running performance of the train. Among them, parameter analysis varies the value of a parameter under the assumption that other parameters remain unchanged to obtain different responses, so that the parameters can be reasonably selected by analyzing the relationship curve between the response and the parameter [17].

Since track stiffness is an important parameter that affects the dynamic characteristics of the wheel-rail system; the purpose of studying LVT stiffness is to optimize the dynamic characteristics of the track under the premise of ensuring the safety and stability of heavy-haul trains [17]. In the design, starting from the track stiffness, the concepts and methods of track structure dynamic design are introduced to reduce or optimize the construction investment; in the maintenance, the existing maintenance procedures are appropriately adjusted around the detection and control of the track stiffness to reduce maintenance investment. In the research of track stiffness, it is necessary to reasonably determine the total track stiffness, the stiffness combination of the various components of the track and find the limit of the rate of change of the track stiffness according to the operating conditions [18,19]. The reasonable value of track stiffness should firstly optimize the dynamic characteristics of the track, and secondly, it should be considered that less investment in construction and maintenance is a complex problem involving a wide range of aspects [20,21].

At present, there are many studies about LVT on high-speed railways and subways, but there are few studies on the heavy-haul railway, and there are fewer references on the dynamic response of track structure parameters to heavy-haul vehicle-track systems [22]. Under such operating conditions, whether LVT can replace ballasted tracks or other types of ballastless tracks, the reasonable stiffness range of the LVT track structure, whether the geometry of the track structure can be maintained under the effect of train load, and whether the safety and comfort of driving can be guaranteed are problems that still need to be researched.

Furthermore, the object of the present study was to investigate traditional speed, acceleration or displacement responses, but system dynamics response sensitivity features are rarely discussed [21]. In light of this, we calculated and compared the system dynamics of the upper heavy-haul vehicle/track system based on system dynamics response sensitivity and vehicle-track coupled dynamics under the influence of different track structure parameters, using LVT on the heavy-haul railway as an example. The appropriate under-rail stiffness and under-block stiffness are suggested from the perspective of system dynamics response sensitivity, in order to provide scientific guidance for the parameter design of LVT on heavy-haul railways in the future.

Based on the existing research on LVT vibration damping mechanism, indoor tests, construction technology, etc. [11–14], we incorporated LVT in a tunnel to focus on the suitable stiffness of this track structure under the operating conditions of a 30 t heavy-haul train. The time domain and frequency domain analysis methods of the wheel-rail system were used in a dynamic analysis to analyze the dynamics effect of the track stiffness based on the analysis of the rule of the track's dynamic parameters with the goal of optimizing LVT dynamic characteristics. Sensitivity to the stiffness of the optimization analysis method was also analyzed to study the value of the total stiffness and the reasonable combination of the stiffness of the heavy-haul railway LVT.

## 2. Heavy-Haul Vehicle-Track Coupled Dynamics Model

### 2.1. Basic Assumptions and Simplified Mechanical Relations

For the purposes of this research, the restraint relationship between the train body structure components were reasonably simplified [21] and the interaction and restraint relationship between the various components in the system were set with the force element and the connection width, so that the mechanical relationship could be simulated. A complex train-vehicle system was abstracted into a simpler multi-body dynamic model, which not only reduces the modeling workload, but also improves the efficiency of model solution analysis. The main application assumptions were as follows:

1. Considering the effect of a single-section vehicle, a 30-t axle heavy-haul coal gondola is running at a constant speed on the track line, ignoring the influence of the lateral wind force and the longitudinal force of the connecting device between the vehicles;
2. The vehicle body has a symmetrical structure along the lateral and longitudinal center lines of the vehicle body, and the center of mass of the vehicle body is the geometric center of the vehicle body;
3. The longitudinal position of the center of mass of the side frames and bolsters is at the geometric center of the bogie; the lateral spacing of the center of mass of the left and right-side frames is the lateral span of the primary and secondary springs;
4. Ignore the influence of the elastic deformation on the structural components of the vehicle system such as the vehicle body, bolster, side frame, and wheel set, and simplify it to a rigid body.

### 2.2. Dynamic Model of Heavy Haul Train

The railway vehicle system modeling generally followed a bottom-up approach to gradually establish rigid components such as wheel sets, crosstie bars, axle boxes, side frames, bolsters, and friction wedges, and establish the relationship between the various structural components with hinges and force elements, so that we were able to complete the modeling of a single bogie and generate a subsystem. By copying the subsystem and establishing the connection between the bogie and the vehicle body through articulation, the train vehicle dynamics modeling process could be completed.

Based on the application of the multi-body system dynamics theory, we used UM (Version 8.5.8.8 64 bit, all rights reserved (c), 1993–2019, Computational Mechanics Ltd., Glinischevo, Bryansk region, Russia) to simulate a 30-t axle load train dynamics model. The most significant advantage of UM software is that it can regard the vehicle body, bolster, side frame, friction wedge and wheel set as ideal rigid bodies, regardless of the influence of their geometric dimensions in the dynamic analysis. In the UM software, a rigid body part was established by importing its geometric drawings, and the mass, center of mass, moment of inertia and other parameters of the structural part are assigned to the rigid body [23,24], as shown in Figure 2.

Table 1 shows the key parameters of the dynamic model of the 30-t axle heavy-haul coal gondola used in this research.

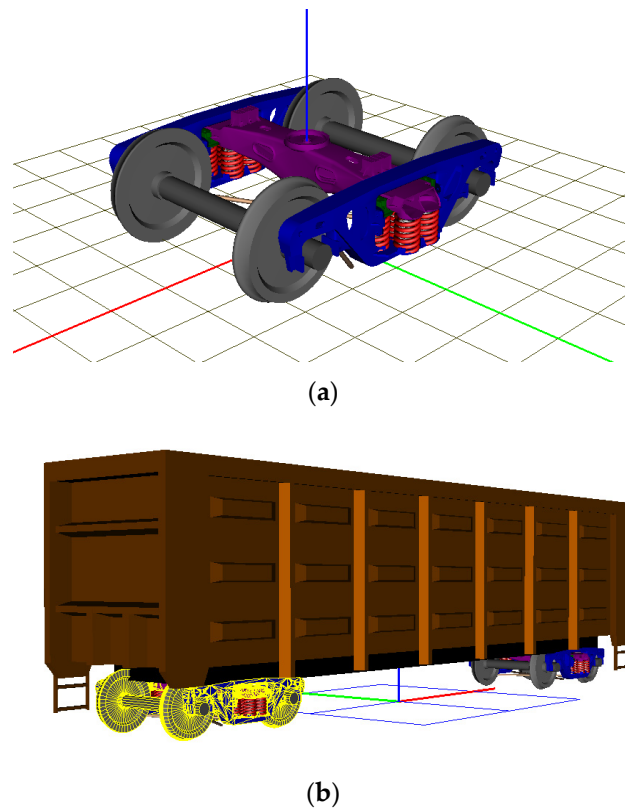


Figure 2. Vehicle dynamics model of heavy haul train. (a) Bogie model and (b) Vehicle body model.

Table 1. Key dynamic model parameters of 30 t axle heavy-haul train.

Name	Unit	Parameter Value
Vehicle body mass	kg	109,200 (Heavy)/13,200 (Light)
Side frame mass	kg	580
The position of the car’s center of gravity (from the rail surface)	z/m	2.155 (Heavy)/1.596 (Light)
The position of the center of gravity of the side frame (from the rail surface)	z/m	0.5135
Bolt mass	kg	680
Wheel set mass	kg	1420
The position of the center of gravity of the bolster (from the rail surface)	z/m	0.515 (Heavy)/0.5625 (Light)

### 2.3. Random Track Irregularity Excitation

Under long-term reciprocating action, random track irregularities will be formed. Common types of track irregularities include four basic forms: level, height, direction, and gauge. In actual operating lines, random track irregularities are the superimposition of the above four basic forms of irregularities. Many countries in the world have determined their own track irregularity power spectral density and related functions based on domestic tracks. Since China started late, it has not yet formed a unified national standard for the power spectrum of track irregularities. Therefore, this paper chooses the American five-level track irregularity spectrum, which is close to the spectrum of China’s three main lines, as the random irregularity excitation of the wheel-rail system.

The UM software can directly call the track irregularity spectrum generation module, select the track spectrum of different countries according to the needs, and select the wavelength range to be analyzed to directly generate the required track irregularity spectrum. When analyzing the dynamic response of the LVT structure in this paper, based on the safety of the track structure itself under more unfavorable track irregularity excitation, the safety coefficient selected is 0.25 when the track irregularity excitation is input. The lateral

and vertical random irregularities of the left and right rails used in the optimization of the track structure stiffness are shown in Figure 3.

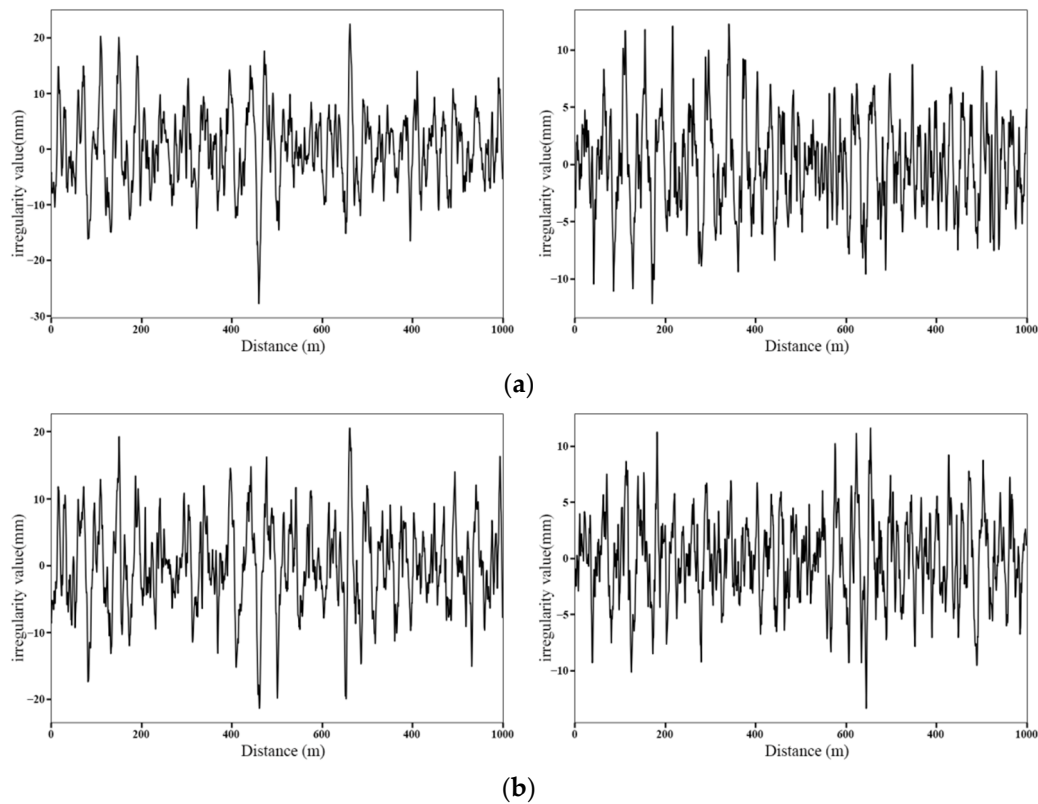


**Figure 3.** A sample of random track irregularities in the U.S. five-level spectrum. (a) Random irregularity samples of the left rail: vertical, lateral (b) Random irregularity samples on the right rail: vertical, lateral.

#### 2.4. Dynamic Model of LVT

LVT structure is mainly composed of rail, elastic VII type fasteners, elastic support blocks, rubber boots and track bed slabs, as shown in Figure 4. In view of the focus of the research question, the track slab mode has little influence on the wheel-rail force during dynamic calculation and analysis, so the track structure can be appropriately simplified.

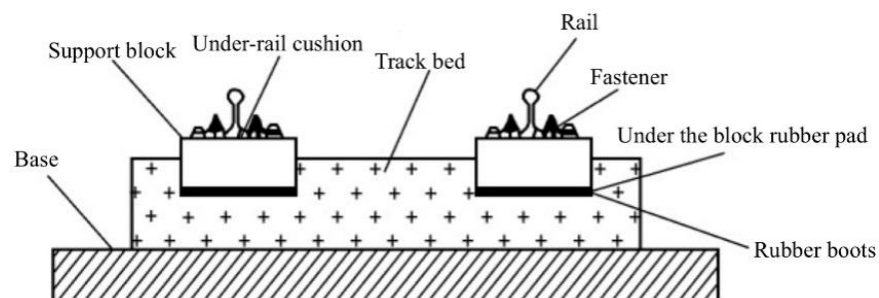


**Figure 4.** The LVT structure.

Figure 5 shows the wheel-rail contact of the simplified rail-elastic support block-based dynamic model of the LVT. Among them, the dynamic modeling of the double-layer track structure is mainly divided into two parts: the rail ① and the LVT structure ③. The rail ① can be regarded as a finite-length Euler–Bernoulli beam on the continuous elastic discrete point ②, which will produce translation and rotation in vertical, lateral and longitudinal directions; the elastic support block ③ is considered a rigid body, which is a discrete support element under rail ①, its translation and rotation in the lateral and vertical directions are also considered; rubber pad under rail ② and the rubber boots ④

under block are considered as spring damping units, respectively connecting the rail ① and the LVT track structure ③, the LVT structure ③ and the foundation ⑤.

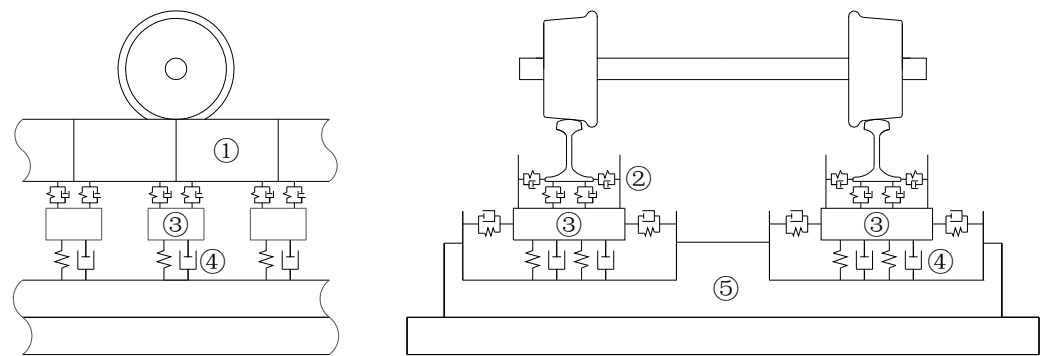


**Figure 5.** Schematic diagram of wheel-rail contact model.

### 2.5. Wheel-Rail Contact Model

The Kik–Piotrowski wheel-rail contact solution method adopted by UM is a contact theory method based on virtual penetration. This method uses only the coordinates of the wheel tread profile in the calculation, which can avoid calculation errors caused by abnormal fluctuations in the curvature of the tread profile, and the dynamics calculation results are more accurate [16]. Compared with the classical Hertz contact theory, the multi-point contact theory can better solve the position and shape of the contact spot of the wheelset and can better describe the change trend of the contact force in the contact spot area. Especially, in the actual operation of the train, under the excitation of track irregularity, the wheel-rail contact force and position change dynamically with time. At certain moments, the wheel-rail contact may change from a single-point contact state to two or even multiple points. Therefore, the theory of multi-point contact is closer to reality and can better describe the contact behavior between the wearing wheel and the rail. Based on the above considerations, the wheel-rail contact model in this paper adopts the Kik–Piotrowski wheel-rail contact solution method.

### 2.6. Description of Operating Conditions of Track Structure Stiffness Analysis

#### 2.6.1. Selection of the Stiffness Range of the Track Structure

The LVT structure adopts the double-layer vibration damping form of the under-rail rubber pad and under-block rubber boots, which can well attenuate the wheel–rail impact and effectively reduce the dynamic damage to the track and basic auxiliary structure. Reasonable track stiffness settings can improve the wheel-rail contact state and increase the safe service life of the track structure. Although the pad with greater static stiffness is beneficial to maintain track geometry, the increase in the stiffness of the pad will also increase the vibration of the track structure, increase the pressure at the sleeper node, and shorten the service life of the pad components. The stiffness of the LVT structure in the lateral direction of the track is mainly provided by the under-rail pad and the elastic rubber boots around the support block to slow down the lateral dynamic impact of the train and maintain the lateral position of the track; the vertical stiffness is mainly determined by the stiffness of the under-rail fastener and the stiffness of the under-block rubber boots and pad.

Although rubber material has a good function of alleviating the impact of the wheel and rail, its fatigue durability and reliability under the reciprocating load of the large axle remain untested. The rubber pad has long been subjected to heavy-haul trains with large axle loads and large volumes of reciprocating effects, and coefficients such as environment, climate, and line conditions have led to fatigue and aging, which greatly shortens its safe service life. Existing investigations of the Daqin heavy-haul railway show that the stiffness value of the under-rail pads can reach 229.1 kN/mm after 5 years of operation and service [25]. Considering that the stiffness characteristics of rubber materials will change

greatly, it is necessary to study the influence of the changes in the stiffness characteristics under the LVT rail and under block of the heavy haul railway on the dynamic performance of the heavy haul train-LVT structure system. Aiming at the double-layer stiffness of the LVT structure, the single-coefficient variable method is adopted to study its influence on the dynamic performance of the rail system. When a certain stiffness is a non-analytical coefficient, its value is selected as the middle value of the value range. The value range and increment of each influencing coefficient are shown in Table 2.

**Table 2.** Optimal values of track structure stiffness (unit: kN/mm).

Influencing Coefficients	Ranges	Value for Non-Variable Coefficients	Increment
Vertical stiffness under rail	80~240	160	20
Lateral stiffness under rail	80~240	160	20
Vertical stiffness under block	40~160	100	20
Lateral stiffness under block	80~240	160	20

### 2.6.2. Comparison and Verification of Heavy Haul Train-LVT Coupled Dynamic Model

In order to verify the rationality of the established 30 t axle heavy-haul vehicle-track coupled dynamics model, this paper compares the existing heavy-haul railway vehicle-track coupled dynamics research results to further enhance the reliability of the conclusions of this paper. For the purpose of this research, in order to better compare and verify the research results of others, this section selects the American five-level spectrum as the track irregularity excitation, and the wheel-rail force when the 30 t axle heavy-haul train runs at 80 km/h is the verification coefficient.

According to Table 3, when the American five-grade track irregularity spectrum excitation is applied, the calculation results in this research are within 10% of the existing reference [26,27]. Taking into account the slightly different values of some parameters of the vehicle track structure, the calculation results in this research are highly reliable.

**Table 3.** Comparison and verification of wheel-rail force (unit: kN).

Comparison Coefficient	References [28,29]	Calculated Value in This Article	Relative Difference (%)
Wheel-rail vertical force	201.1	193.2	4.19
Wheel-rail lateral force	52.1	48.3	7.87

## 3. Research on the Influence of Track Structure Stiffness Change on the Stability of Vehicle

### 3.1. Vertical Stiffness under Rail

According to the calculation results of the simulation conditions of different vertical stiffness under rail, the maximum values of vehicle body lateral acceleration, vehicle body vertical acceleration, wheel-rail vertical force, wheel-rail lateral force, derailment coefficient, and wheel load reduction rate are summarized in Table 4 and the changes are shown in Figure 6.

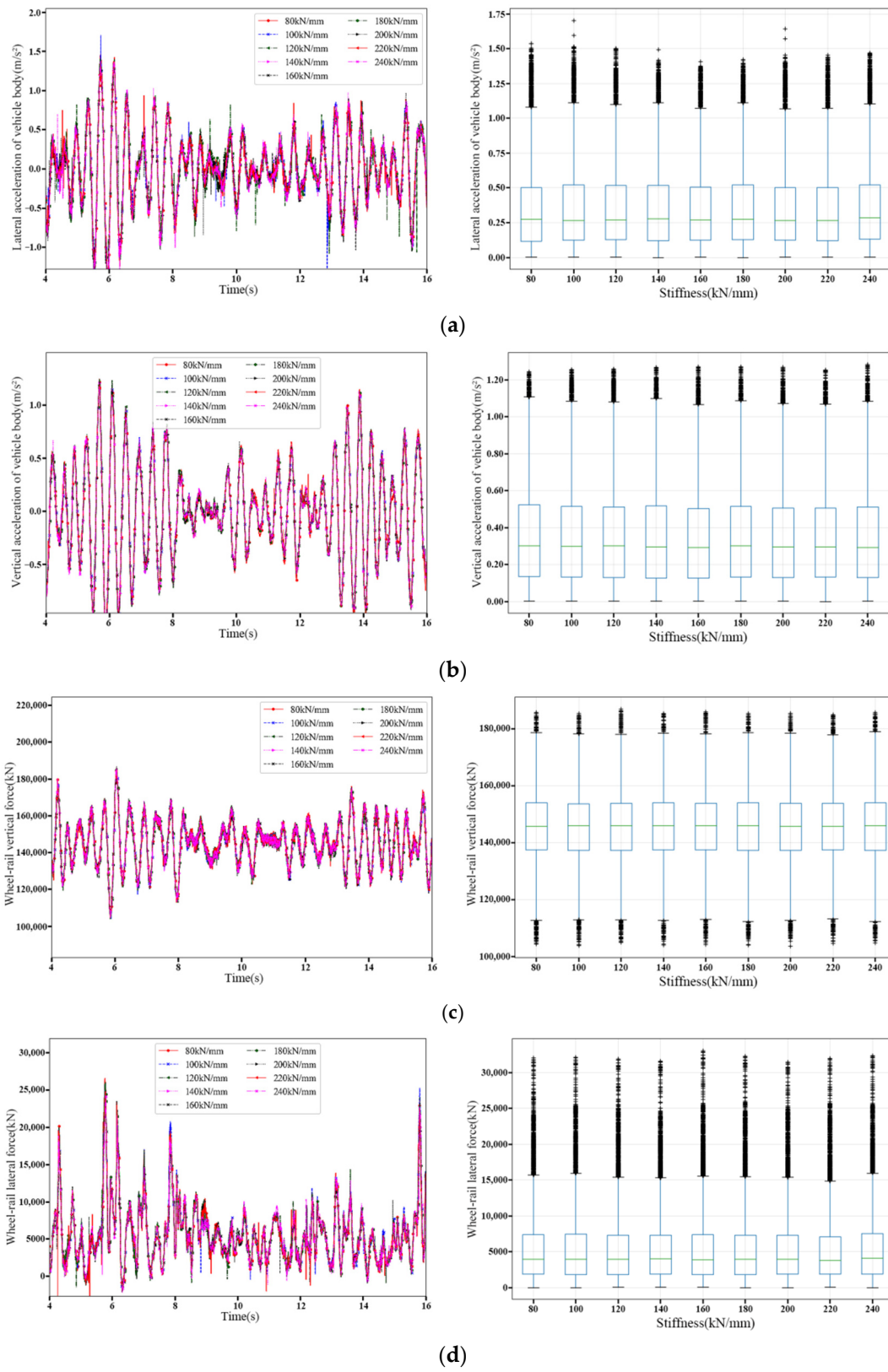
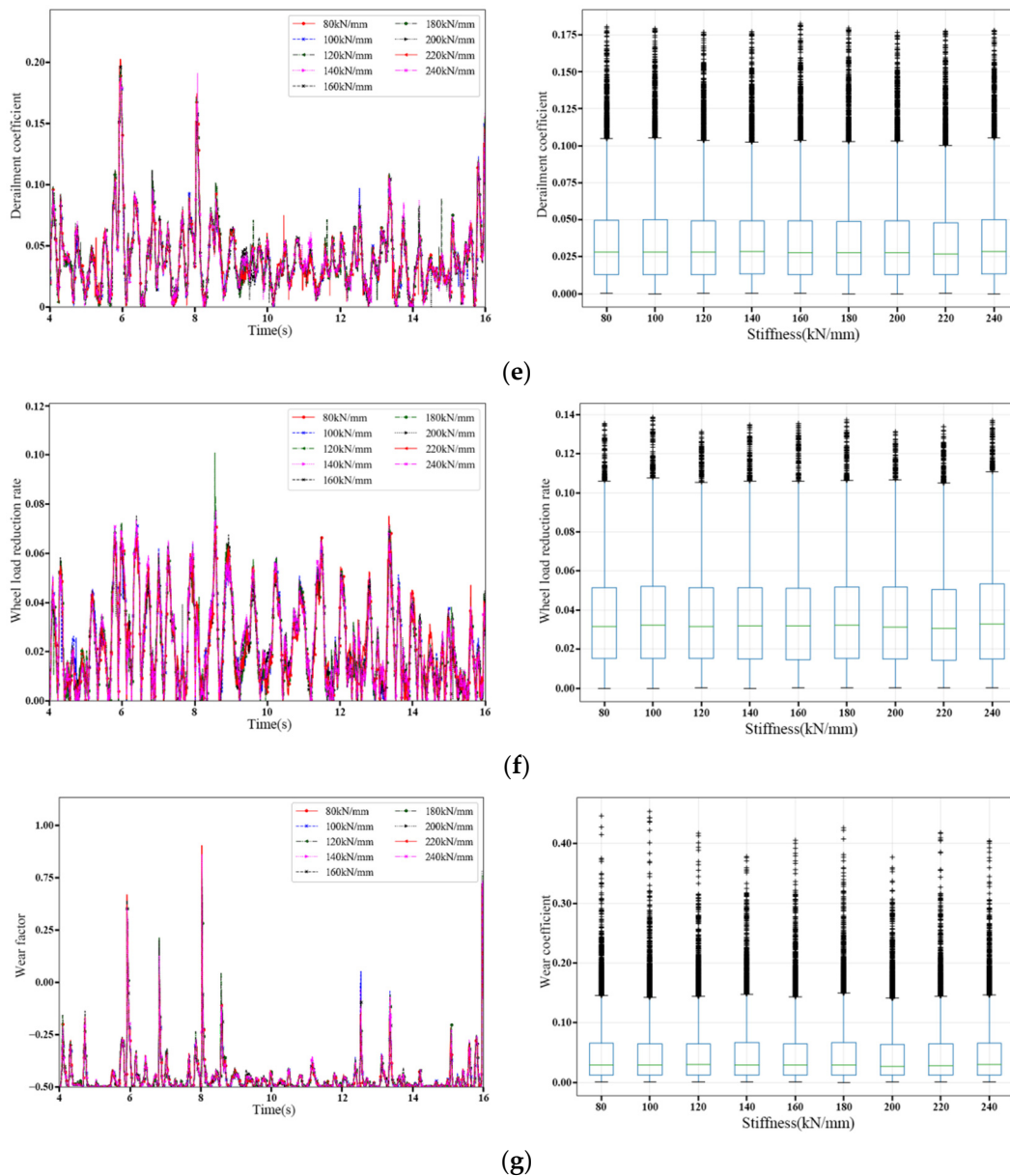


Figure 6. Cont.



**Figure 6.** Variations in the stability coefficient under different vertical stiffness under rail. (a) Vehicle body lateral acceleration change: left-time history waveform, right-maximum, (b) Vehicle body vertical acceleration change: left-time history waveform, right-maximum, (c) wheel-rail vertical force change: left-time history curve, right-statistical distribution, (d) wheel-rail lateral force change: left-time history curve, right-statistical distribution, (e) Deraulment coefficient change: left-time history curve, right-statistical distribution, (f) Wheel load shedding rate change: left-time history curve, right-statistical distribution and (g) Wear coefficient change: left-time history curve, right-statistical distribution.

The right graphs of Figure 6 are box diagrams drawn according to the change curve of each dynamic response coefficient. The box diagrams can be used to easily view the original distribution of discrete data. The upper and lower lines of the rectangular box represent the upper and lower quartile values of the data, the lateral line in the rectangular box represents the median of the data, and the upper and lower lateral lines, respectively, represent the maximum and minimum values calculated based on the quartile values, and the rest are marked as out-of-boundary numerical points.

In order to ensure the safety of train operation, China’s “Railway vehicles-specification for evaluating the dynamic performance and accreditation test”, based on the vibration intensity of the train body, sets limits on the lateral and vertical acceleration of the vehicle

body, and requires the lateral and vertical acceleration of vehicle body, respectively, no more than 0.5 g, 0.7 g. The article uses these limits as the reference limits for the study [26].

According to the analysis of Table 4 and Figure 6, when the vertical support stiffness under rail changes within the range of 80~240 kN/mm, the lateral and vertical acceleration of vehicle body varies in the range of 1.397~1.702 m/s<sup>2</sup>, 1.175~1.243 m/s<sup>2</sup>; none of them exceed the limits of the lateral acceleration and vertical acceleration of the “Railway vehicles-specification for evaluating the dynamic performance and accreditation test”. The maximum wheel-rail vertical force and wheel-rail lateral force vary with the vertical support stiffness under the rail in 184.5~186.9 kN, 31.5~33.0 kN, and the relative change rates are 1.32% and 4.76%, indicating that the wheel-rail vertical force and the lateral force is not significantly affected by the change of the vertical support stiffness under the rail, and the changes of the two are basically the same; the maximum range of derailment coefficient, wheel load reduction rate, and wear coefficient are 0.189~0.202, 0.131~0.139, 2.040~2.306, and the relative change rates are, respectively, 6.88%, 5.68%, 13.04%.

**Table 4.** Summary table of maximum values of stability control coefficient for train and vehicle.

Vertical stiffness under rail (kN/mm)	80	100	120	140	160	180	200	220	240
Lateral acceleration (m/s <sup>2</sup> )	1.537	1.702	1.399	1.397	1.408	1.425	1.573	1.439	1.453
Vertical acceleration (m/s <sup>2</sup> )	1.243	1.223	1.240	1.209	1.215	1.201	1.207	1.187	1.175
wheel-rail vertical force (kN)	185.8	185.3	186.9	185.3	184.5	185.5	185.5	185.0	185.9
wheel-rail lateral force (kN)	32.0	32.1	31.9	31.6	32.1	32.3	31.5	31.9	32.3
Derailment coefficient	0.202	0.194	0.189	0.190	0.198	0.194	0.189	0.190	0.191
Wheel load reduction rate	0.135	0.139	0.131	0.135	0.132	0.137	0.131	0.134	0.137
Wear coefficient	2.193	2.183	2.089	2.040	2.392	2.191	2.068	2.306	2.219

### 3.2. Lateral Stiffness under Rail

According to the calculation results of the simulation conditions of different lateral stiffness under rail, the maximum values of vehicle body lateral acceleration, vehicle body vertical acceleration, wheel-rail vertical force, wheel-rail lateral force, derailment coefficient, and wheel load reduction rate are summarized in Table 5, the changes are shown in Figure 7.

**Table 5.** Summary table of maximum value of train vehicle stability control coefficients.

Lateral stiffness under rail (kN/mm)	80	100	120	140	160	180	200	220	240
Lateral acceleration (m/s <sup>2</sup> )	1.370	1.440	1.700	1.550	1.740	1.400	1.390	1.520	1.640
Vertical acceleration (m/s <sup>2</sup> )	1.190	1.210	1.230	1.230	1.190	1.200	1.220	1.270	1.200
wheel-rail vertical force (kN)	185.0	186.0	185.0	185.0	185.0	185.0	186.0	186.0	186.0
wheel-rail lateral force (kN)	31.0	32.3	32.9	32.4	31.8	31.8	31.8	32.6	32.2
Derailment coefficient	0.182	0.197	0.206	0.194	0.189	0.191	0.193	0.200	0.196
Wheel load reduction rate	0.133	0.132	0.135	0.137	0.138	0.137	0.129	0.138	0.135
Wear coefficient	2.180	2.280	2.160	2.130	2.080	2.180	2.080	2.190	2.150

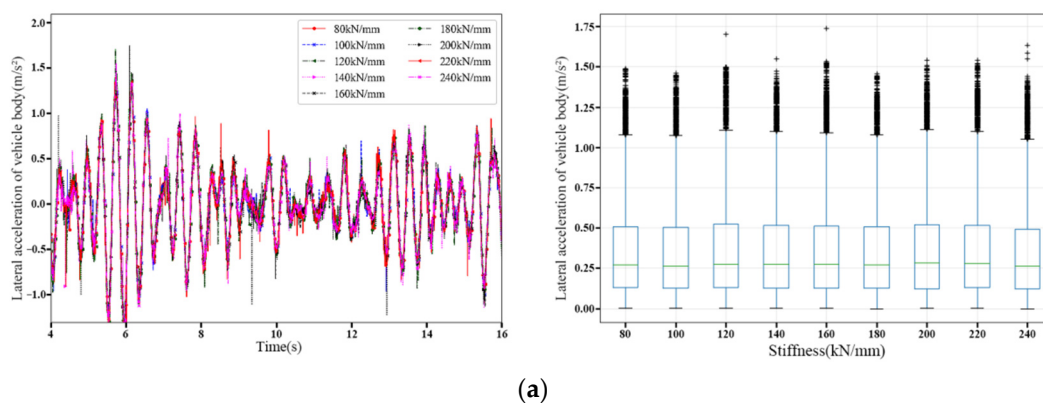


**Figure 7.** Cont.

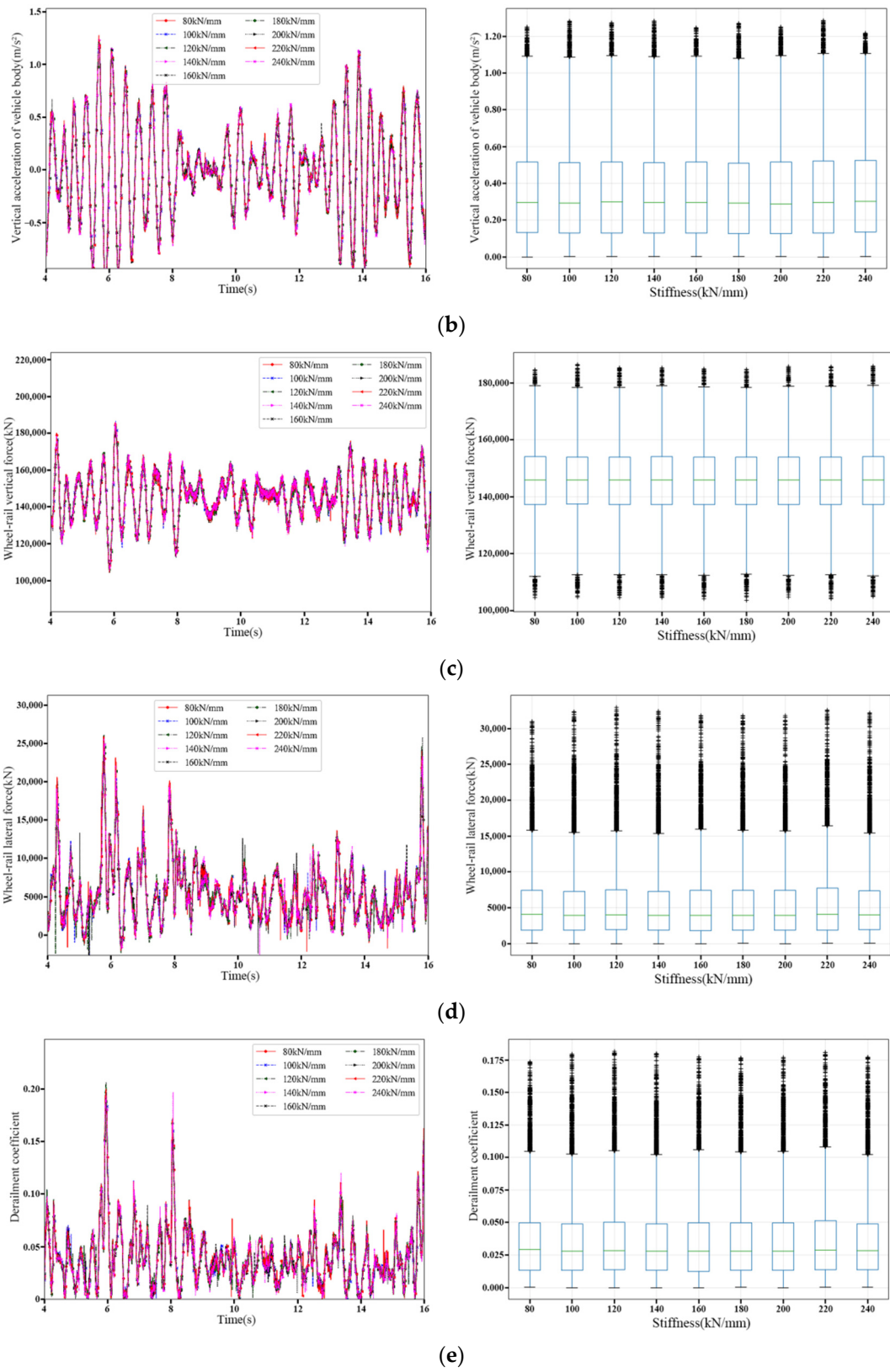
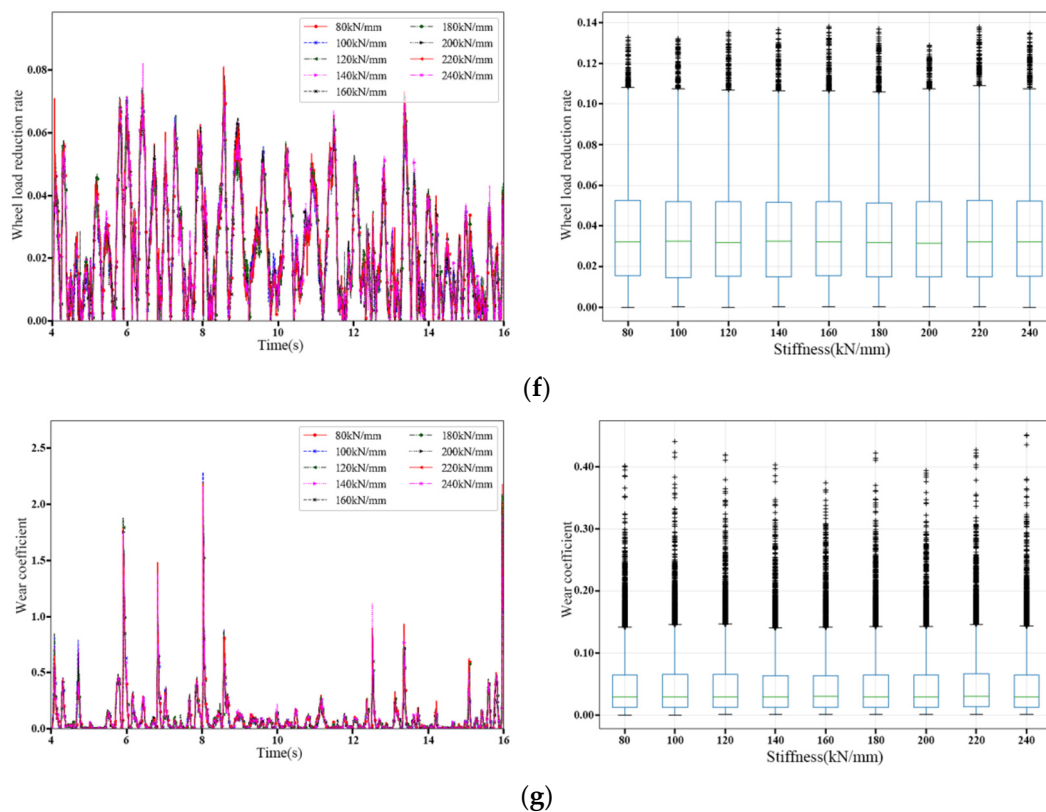


Figure 7. Cont.



**Figure 7.** Variations in the stability coefficient under different lateral stiffness under rail. (a) Vehicle body lateral acceleration change: left-time history waveform, right-maximum, (b) Vehicle body vertical acceleration change: left-time history waveform, right-maximum, (c) wheel-rail vertical force change: left-time history curve, right-statistical distribution, (d) wheel-rail lateral force change: left-time history curve, right-statistical distribution, (e) Derailment coefficient change: left-time history curve, right-statistical distribution, (f) Wheel load shedding rate change: left-time history curve, right-statistical distribution and (g) Wear coefficient change: left-time history curve, right-statistical distribution.

According to the analysis in Table 5 and Figure 7, when the vertical support stiffness under rail changes in the range of 80~240 kN/mm, the lateral and vertical acceleration of the train body changes in the range of 1.370~1.740 m/s<sup>2</sup> and 1.190~1.270 m/s<sup>2</sup>, respectively, the relative change rate is 27.01% and 6.72%, respectively, and the lateral and vertical acceleration of the vehicle body are within the specified limits. The maximum values of wheel-rail vertical force and wheel-rail lateral force vary with the lateral support stiffness under the rail to 185.0~186.0 kN, 31.0~32.9 kN, and the relative rate of change is 0.54% and 6.13%. The maximum range of derailment coefficient, wheel load reduction rate and wear coefficient are 0.182~0.206, 0.129~0.138, 2.075~2.285, and the relative change rates are 13.19%, 7.23%, 10.09%, respectively. The amplitudes of various control coefficients of driving safety are all within the limit. Therefore, when the rigidity of the lateral support under the rail increases, the maximum value of wheel-rail vertical force, lateral force, and wheel load reduction rate does not change significantly.

### 3.3. Vertical Stiffness under Block

According to the calculation results of the simulation conditions of different vertical stiffness under block, the maximum values of vehicle body lateral acceleration, vehicle body vertical acceleration, wheel-rail vertical force, wheel-rail lateral force, derailment coefficient, and wheel load reduction rate are summarized in Table 6, the changes are shown in Figure 8.

**Table 6.** Summary table of maximum value of train vehicle stability control coefficients.

Vertical stiffness under block (kN/mm)	40	60	80	100	120	140	160
Lateral acceleration (m/s <sup>2</sup> )	1.534	1.451	1.404	1.42	1.381	1.437	1.528
Vertical acceleration (m/s <sup>2</sup> )	1.236	1.238	1.206	1.235	1.210	1.20	1.215
wheel-rail vertical force (kN)	185.7	185.8	185.0	185.4	185.3	185.6	185.4
wheel-rail lateral force (kN)	31.5	32.0	31.7	31.0	32.1	31.9	32.6
Derailment coefficient	0.200	0.194	0.192	0.192	0.189	0.199	0.192
Wheel load reduction rate	0.132	0.136	0.128	0.128	0.136	0.136	0.135
Wear coefficient	2.142	2.139	2.073	2.115	2.092	2.129	2.288

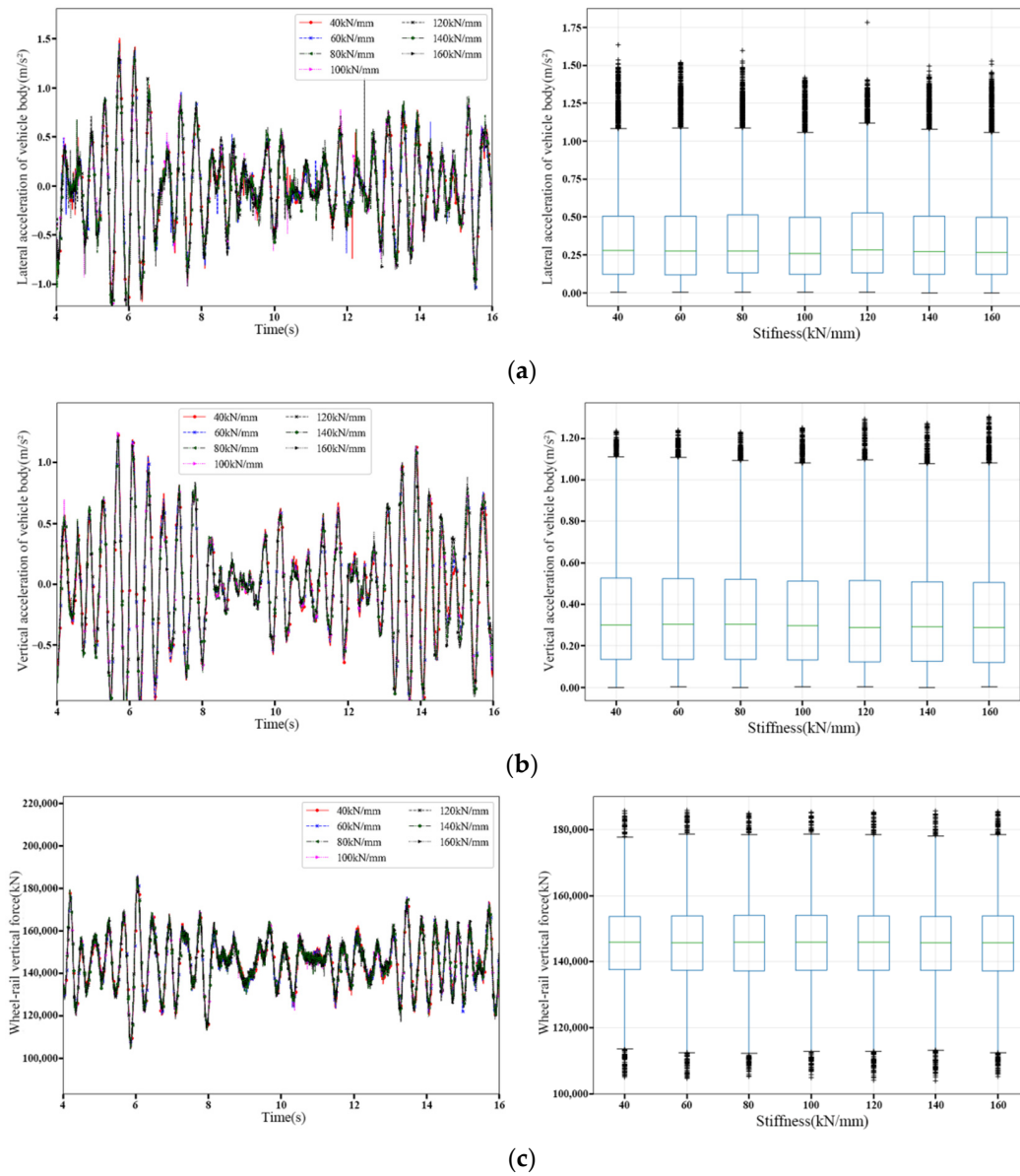


**Figure 8.** Cont.

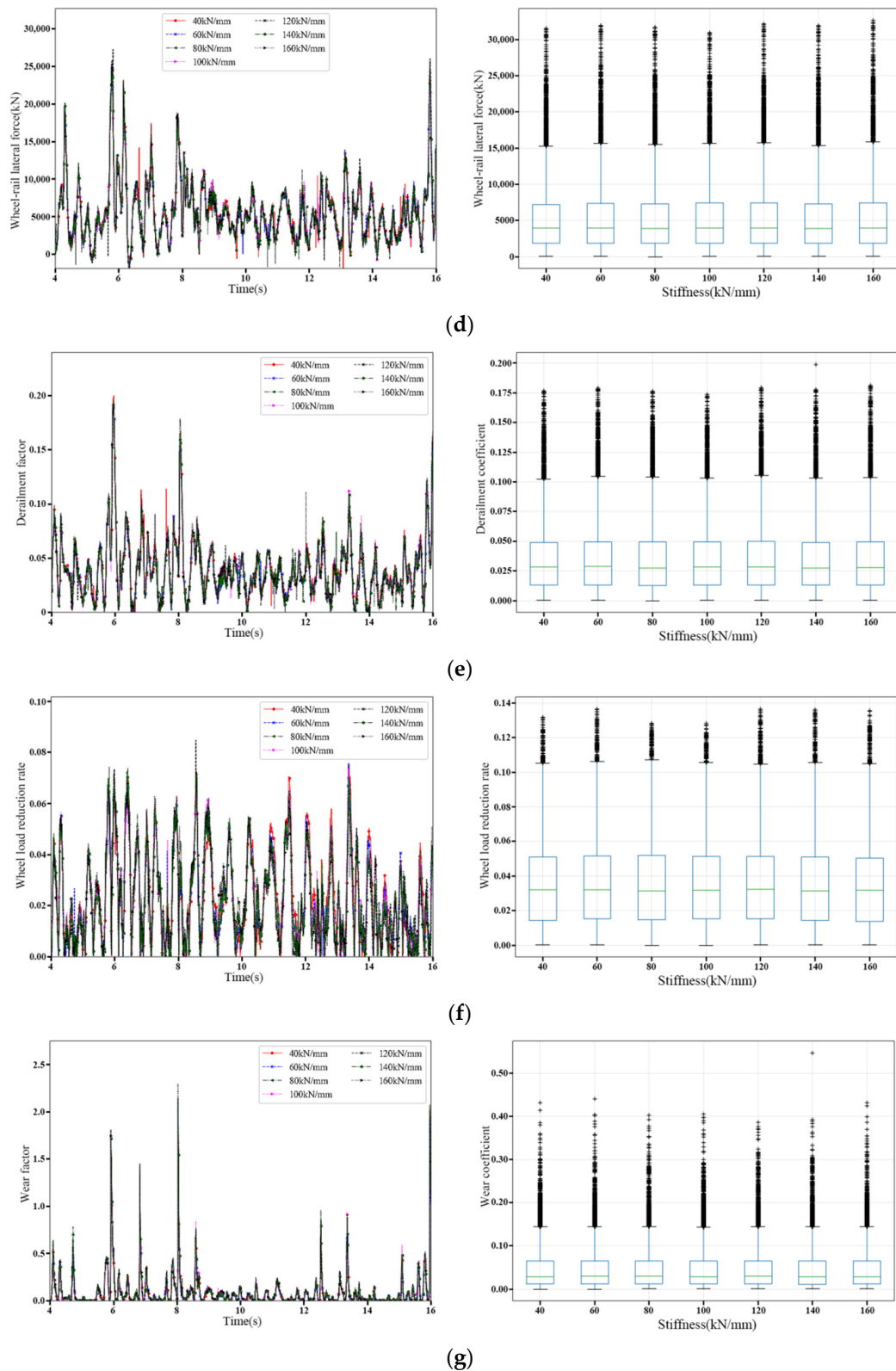


**Figure 8.** Variations in the stability coefficients under different vertical stiffness under block. (a) Vehicle body lateral acceleration change: left-time history waveform, right-maximum, (b) Vehicle body vertical acceleration change: left-time history waveform, right-maximum, (c) wheel-rail vertical force change: left-time history curve, right-statistical distribution, (d) wheel-rail lateral force change: left-time history curve, right-statistical distribution, (e) Derailment coefficient change: left-time history curve, right-statistical distribution, (f) Wheel load shedding rate change: left-time history curve, right-statistical distribution and (g) Wear coefficient change: left-time history curve, right-statistical distribution.

According to the analysis in Table 6 and Figure 8, when the vertical support stiffness under block changes within the range of 80~240 kN/mm, the lateral and vertical acceleration of the train body changes in the range of 1.381~1.534 m/s<sup>2</sup> and 1.200~1.238 m/s<sup>2</sup>, respectively. The relative change rate is 11.08% and 3.17%, respectively, and the lateral and vertical acceleration of the vehicle body are both within the specified limits. The maximum values of wheel-rail vertical force, wheel-rail lateral force, derailment coefficient, wheel load reduction rate, and wear coefficient vary with the vertical support stiffness under block in 185.0~185.8 kN, 31.0~32.6 kN, 0.189~0.200, 0.128~0.136, respectively. The relative change rates were 0.45%, 5.29%, 5.42%, 6.29%, 10.34%, respectively.

### 3.4. Lateral Stiffness under Block

According to the calculation results of the simulation conditions of different lateral stiffness under block, the maximum values of vehicle body lateral acceleration, vehicle body vertical acceleration, wheel-rail vertical force, wheel-rail lateral force, derailment coefficient, and wheel load reduction rate are summarized in Table 7, the changes are shown in Figure 9.

**Table 7.** Summary table of maximum value of train vehicle stability control coefficients.

Lateral stiffness under block (kN/mm)	80	100	120	140	160	180	200	220	240
Lateral acceleration (m/s <sup>2</sup> )	1.534	1.451	1.404	1.42	1.381	1.437	1.528	1.534	1.451
Vertical acceleration (m/s <sup>2</sup> )	1.236	1.238	1.206	1.235	1.210	1.20	1.215	1.236	1.238
wheel-rail vertical force (kN)	185.8	186.1	184.9	185.3	184.4	185.2	185.3	185.5	185.0
wheel-rail lateral force (kN)	31.9	32.1	31.7	32.1	32.2	32.5	32.2	31.9	31.8
Derailment coefficient	0.188	0.183	0.193	0.198	0.193	0.200	0.192	0.187	0.192
Wheel load reduction rate	0.135	0.136	0.131	0.132	0.135	0.132	0.133	0.132	0.134
Wear coefficient	2.132	2.166	2.139	2.159	2.072	2.034	2.102	2.161	2.143

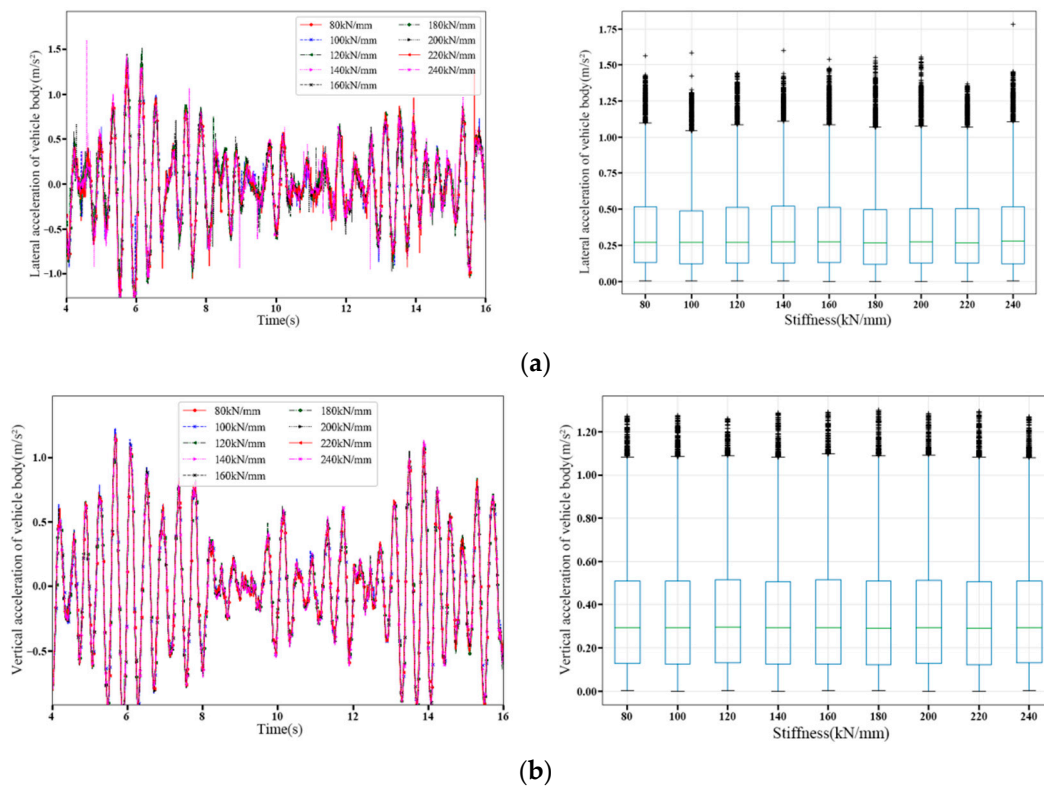


**Figure 9.** Cont.

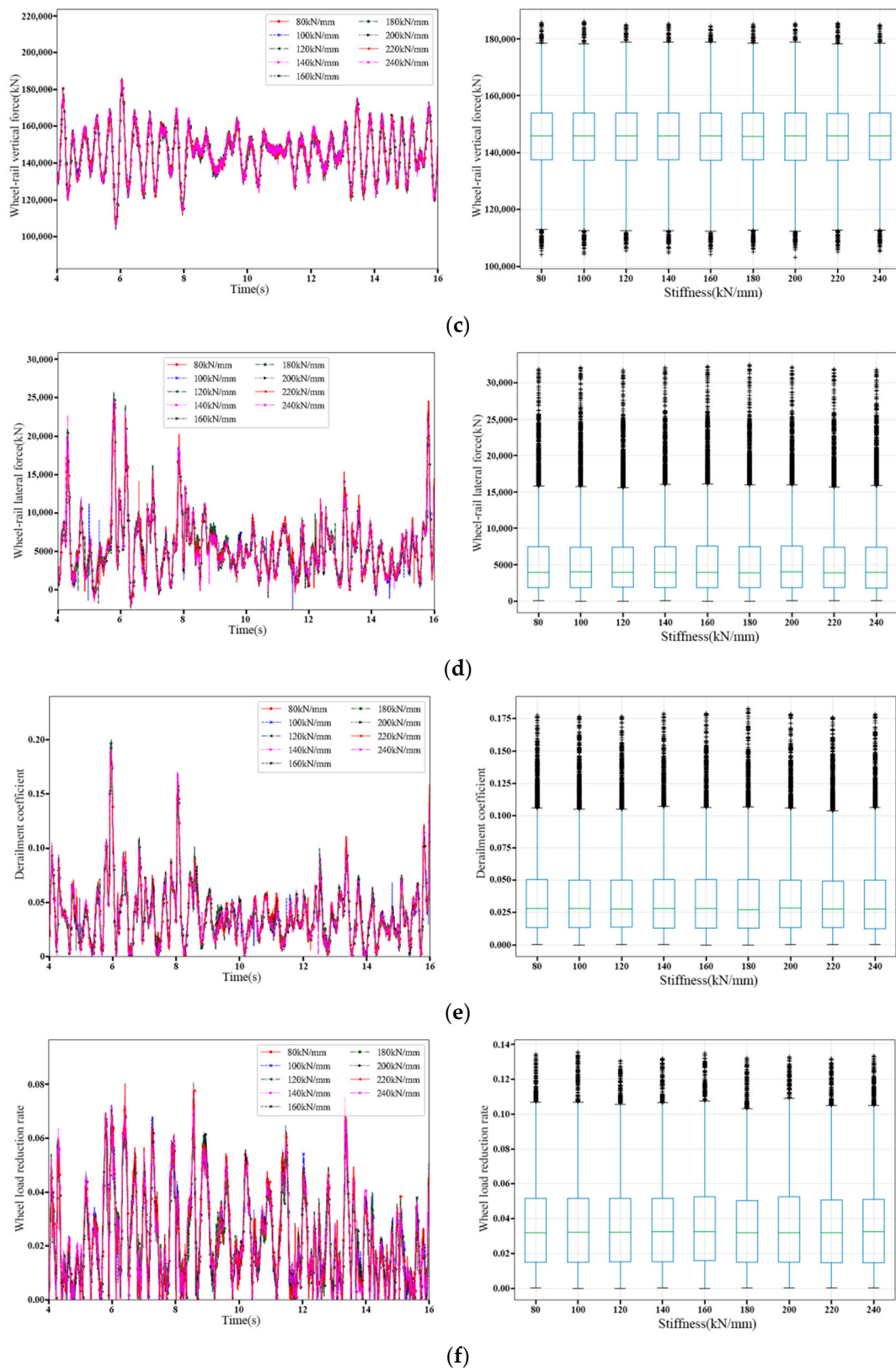
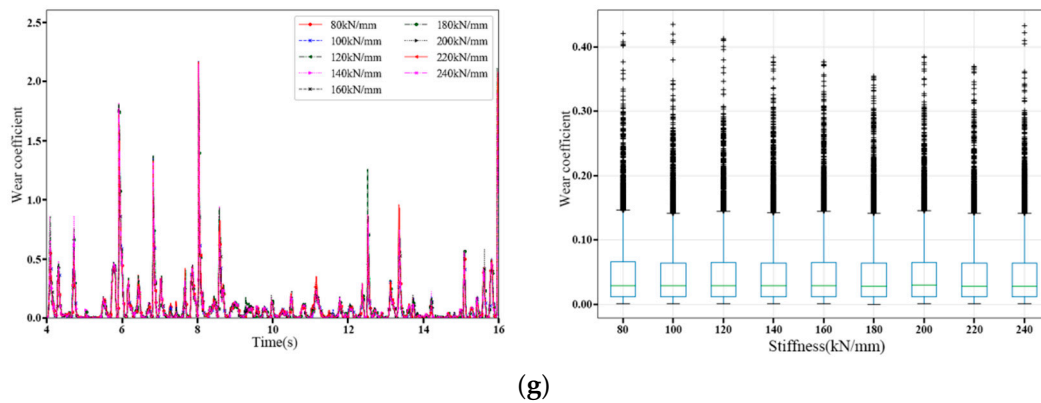


Figure 9. Cont.



**Figure 9.** Variations in the stability coefficients under different lateral stiffness under block. (a) Vehicle body lateral acceleration change: left-time history waveform, right-maximum, (b) Vehicle body vertical acceleration change: left-time history waveform, right-maximum, (c) wheel-rail vertical force change: left-time history curve, right-statistical distribution, (d) wheel-rail lateral force change: left-time history curve, right-statistical distribution, (e) Derailment coefficient change: left-time history curve, right-statistical distribution, (f) Wheel load shedding rate change: left-time history curve, right-statistical distribution and (g) Wear coefficient change: left-time history curve, right-statistical distribution.

According to the analysis in Table 7 and Figure 9, when the lateral support stiffness under block changes within the range of 80~240 kN/mm, the lateral and vertical acceleration of the train body changes in the range of 1.381~1.534 m/s<sup>2</sup>, 1.206~1.238 m/s<sup>2</sup>, the relative change rates are 11.08% and 2.65%, respectively, and the lateral and vertical acceleration of the vehicle body are both within the specified limits. The maximum value of wheel-rail vertical force, wheel-rail lateral force, derailment coefficient, wheel load reduction rate and wear coefficient vary with the stiffness of the lateral support under the block in 184.4~186.1 kN, 31.7~32.5 kN, 0.183~0.200, 0.131~0.136, 2.034~2.166, respectively. The rates of change were 0.93%, 2.36%, 9.15%, 3.91%, 6.51% and the amplitudes of various control coefficients for driving safety were all within the specification limits. When the stiffness of the lateral support under the block increases, the maximum amplitude of the wheel-rail vertical force, lateral force, and wheel load reduction rate does not change significantly.

#### 4. Research on the Influence of Track Structure Stiffness Change on Track Deformation

##### 4.1. Vertical Stiffness under Rail

According to the calculation results of the simulation conditions of different vertical stiffness under rail, the maximum values of the vertical displacement of the rail, the lateral displacement of the rail, and the gauge expansion are summarized in Table 8, the changes are shown in Figure 10.

**Table 8.** Summary table of maximum values of track structure deformation control coefficients.

Vertical stiffness under rail (kN/mm)	80	100	120	140	160	180	200	220	240
Vertical displacement (mm)	1.741	1.591	1.503	1.419	1.367	1.320	1.29	1.255	1.239
Lateral displacement (mm)	0.978	0.969	0.960	0.940	1.003	0.964	0.932	0.947	0.973
Gauge expansion (mm)	0.135	0.139	0.131	0.135	0.136	0.137	0.131	0.134	0.137

According to Table 8, when the vertical support stiffness under the rail increases from 80 kN/mm to 240 kN/mm, the vertical displacement of the rail shows a slow decrease trend. When the vertical support stiffness under the rail increases to a certain value, the vertical displacement of the rail is slightly lowered again. When the vertical support stiffness under rail changes in the range of 80~240 kN/mm, the range of vertical displacement, lateral displacement and gauge expansion of rail are 1.239~1.741 mm, 0.932~1.003 mm, 1.650~1.762 mm, respectively. The relative change rates are 40.48%, 7.66%, 6.73%, respectively; the lateral and vertical displacement of the rail and the amplitude of the gauge expansion are all within the specified limits; the vertical displacement of the rail changes

more obvious, and the lateral displacement and the gauge expansion of the rail change synchronously, but the tendency of change with the stiffness is not significant, indicating that the torsional displacement angle of the rail changes little. In order to maintain the straightness of the vertical position of the track structure, the rigidity of the vertical support under the rail can be appropriately increased, but beyond a certain range, the effect of this measure will be significantly weakened.

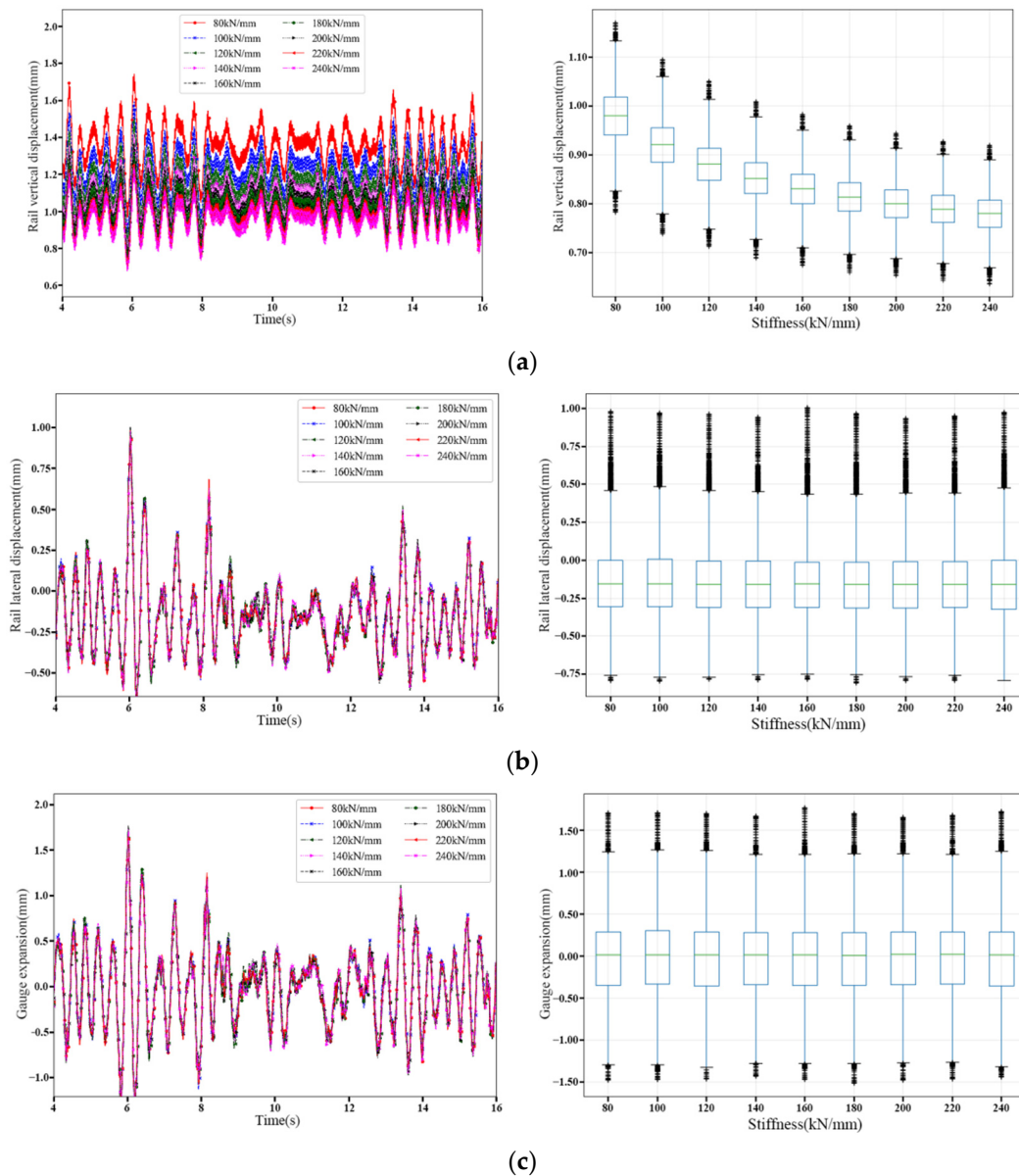


**Figure 10.** Variations in the deformation coefficients under different vertical stiffness under rail. (a) Wheel-rail vertical displacement change: left-time history waveform, right-maximum, (b) Wheel-rail lateral displacement change: left-time history waveform, right-maximum and (c) Change in gauge expansion: left-time history curve, right-statistical distribution.

According to the analysis in Figure 10, it can be seen that the change trend of the rail displacement control coefficients with the vertical support stiffness under the rail is basically the same, and the vertical displacement changes more significantly. According to the analysis of the maximum value curve of each displacement coefficients, the maximum value of rail displacement under different vertical support stiffness under the rail decreases with the increase in the vertical support stiffness under the rail, and the trend gradually slows down. The change tendency of the rail lateral displacement and gauge expansion is not obvious. It shows that under the excitation of random track irregularities, the vertical

stiffness under rail has a greater impact on the vertical displacement of the rail, but has only a slight impact on the lateral displacement of the rail and the expansion of the gauge.

#### 4.2. Lateral Stiffness under Rail

According to the calculation results of the simulation conditions of different lateral stiffness under rail, the maximum values of the vertical displacement of the rail, the lateral displacement of the rail, and the gauge expansion are summarized in Table 9, the changes are shown in Figure 11.

**Table 9.** Summary table of maximum values of track structure deformation control coefficients.

Vertical stiffness under rail (kN/mm)	80	100	120	140	160	180	200	220	240
Vertical displacement (mm)	1.360	1.370	1.360	1.360	1.360	1.360	1.370	1.370	1.370
Lateral displacement (mm)	0.984	1.010	1.030	1.000	0.952	0.944	0.920	0.957	0.938
Gauge expansion (mm)	1.740	1.770	1.790	1.760	1.690	1.670	1.620	1.670	1.650

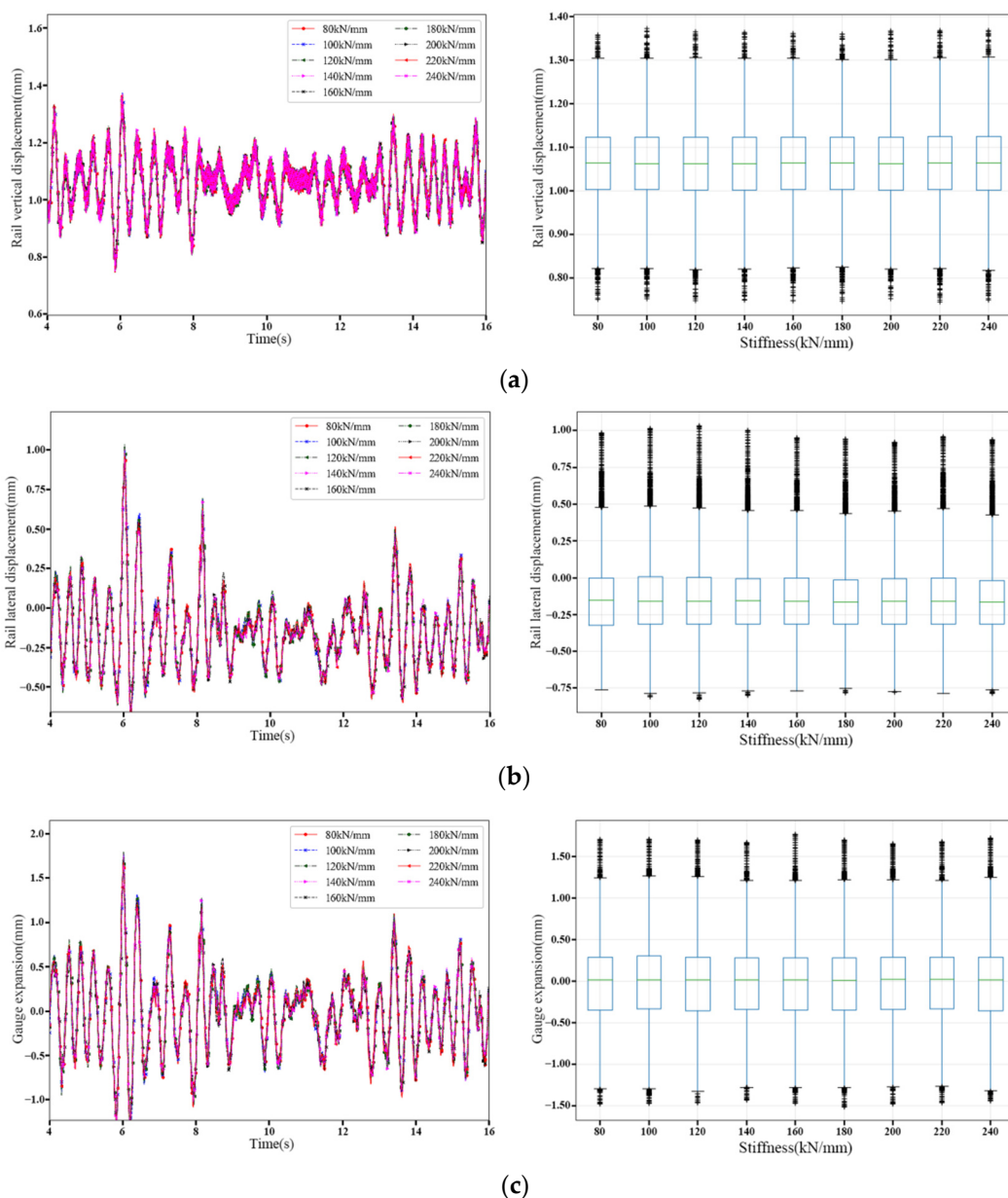


**Figure 11.** Variations in the deformation coefficients under different lateral stiffness under rail. (a) Wheel-rail vertical displacement change: left-time history waveform, right-maximum, (b) Wheel-rail lateral displacement change: left-time history waveform, right-maximum and (c) Change in gauge expansion: left-time history curve, right-statistical distribution.

According to Table 9 and Figure 11, when the lateral support stiffness under the rail is increased from 80 kN/mm to 240 kN/mm, the vertical displacement of the rail changes less, and the lateral displacement and gauge expansion are reduced accordingly. The range of amplitude changes are 0.92~1.032 mm, 1.625~1.788 mm. The relative change rates are 12.16% and 10.02%. The lateral and vertical displacement of the rail and the amplitude of the gauge expansion are all within the specified limits. In order to avoid overturning the steel rail during the running of the heavy-haul train and maintain the smoothness of the gauge, the rigidity of the lateral support under the rail can be appropriately increased. However, it should be noted that the effect of this measure will gradually weaken as the stiffness increases.

#### 4.3. Vertical Stiffness under Block

According to the calculation results of the simulation conditions of different vertical stiffness under block, the maximum values of the vertical displacement of the rail, the lateral displacement of the rail, and the gauge expansion are summarized in Table 10, the changes are shown in Figure 12.

**Table 10.** Summary table of maximum values of track structure deformation control coefficients.

Vertical stiffness under rail (kN/mm)	40	60	80	100	120	140	160
Vertical displacement (mm)	2.268	1.775	1.516	1.365	1.26	1.179	1.127
Lateral displacement (mm)	0.937	0.966	0.94	0.908	0.97	0.955	0.993
Gauge expansion (mm)	1.655	1.708	1.656	1.603	1.714	1.676	1.745

According to Table 10, when the vertical support stiffness under the block increases from 40 kN/mm to 160 kN/mm, the vertical displacement of the rail shows a decreasing trend, and the trend gradually slows down. When the vertical support stiffness under the block increases to a certain value, the vertical displacement of the rail is almost no longer reduced; the ranges of vertical displacement, lateral displacement and gauge expansion of the rail are 1.127~2.268 mm, 0.908~0.993 mm, 1.603~1.745 mm, and the relative change rates are 101.13%, 9.29%, 8.86%, respectively; the lateral and vertical displacement of the rail and the amplitude of the gauge expansion are all within the specified limits. When the vertical stiffness under the block is 40 kN/mm, the vertical displacement of the rail is close to the limit.

According to the analysis in Figure 12, the vertical displacement of the rail gradually decreases with the stiffness of the vertical support under the block, and the lateral displacement and gauge expansion show a certain randomness, but the overall trend is increasing. In order to maintain the straightness of the vertical position of the track structure, the deformation of the rubber boots at the bottom of the support block are reduced, the safe service life of the rubber boots is extended, and the stiffness of the vertical support under the block is appropriately increased.

#### 4.4. Lateral Stiffness under Block

According to the calculation results of the simulation conditions of different lateral stiffness under block, the maximum values of the vertical displacement of the rail, the lateral displacement of the rail, and the gauge expansion are summarized in Table 11, the changes are shown in Figure 13.

According to Table 11 and Figure 13, when the lateral support stiffness under the block increases from 80 kN/mm to 240 kN/mm, the vertical displacement of the rail changes little, and the lateral displacement and gauge expansion change simultaneously, and then show a decreasing trend. The range of amplitude change is 0.933~1.129 mm, 1.659~1.773 mm, and the relative change rates are 9.49%, 6.87%, respectively. The lateral and vertical displacement of the rail and the amplitude of the gauge expansion are all within the specified limits.

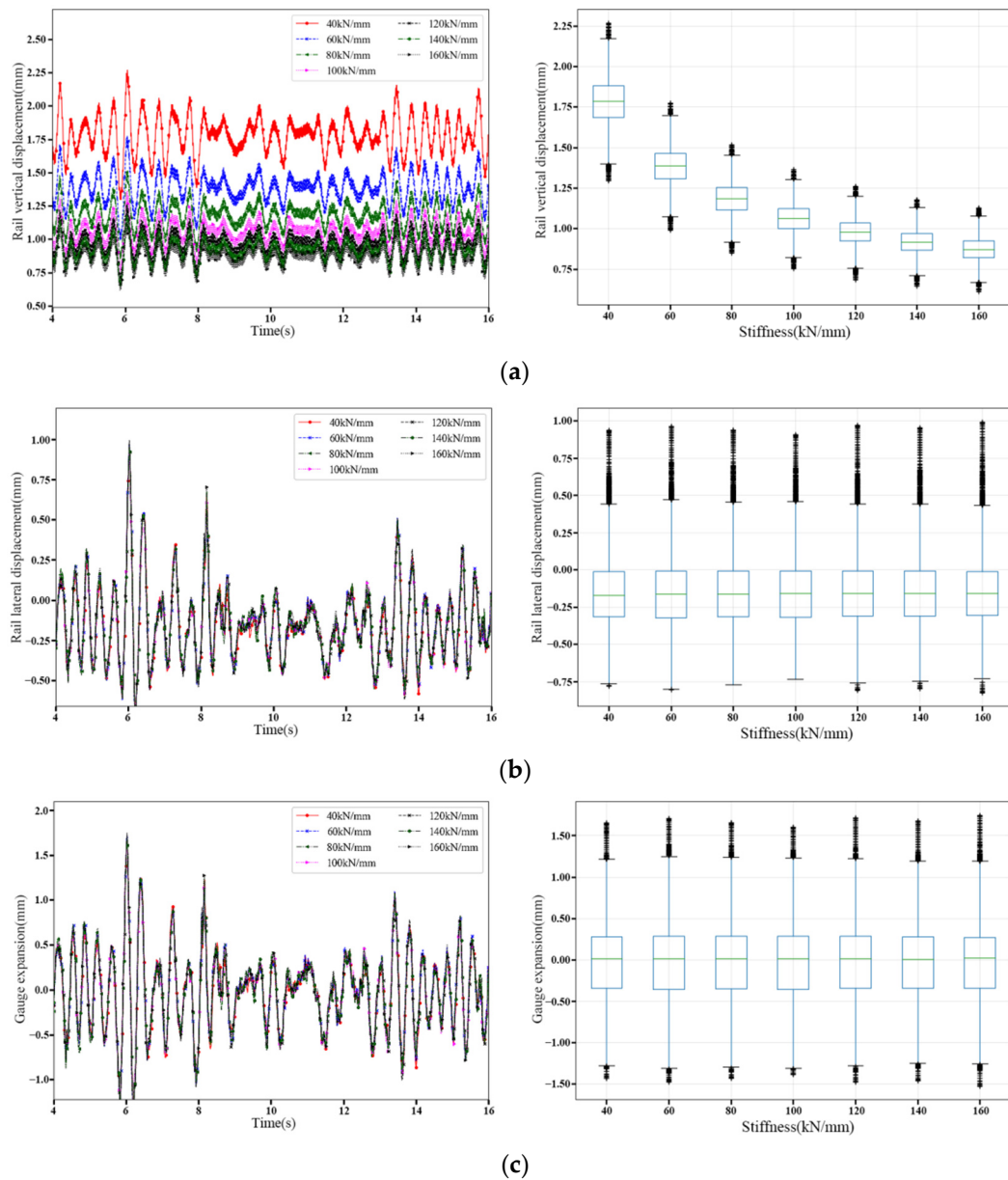


**Figure 12.** Variations in the deformation coefficients under different vertical stiffness under block. (a) Wheel-rail vertical displacement change: left-time history waveform, right-maximum, (b) Wheel-rail lateral displacement change: left-time history waveform, right-maximum and (c) Change in gauge expansion: left-time history curve, right-statistical distribution.

**Table 11.** Summary table of maximum values of track structure deformation control coefficients.

Vertical stiffness under rail (kN/mm)	80	100	120	140	160	180	200	220	240
Vertical displacement (mm)	1.128	1.128	1.125	1.125	1.122	1.124	1.127	1.129	1.127
Lateral displacement (mm)	1.021	1.015	0.964	0.978	0.973	0.974	0.955	0.933	0.934
Gauge expansion (mm)	1.763	1.773	1.683	1.707	1.708	1.710	1.689	1.661	1.659

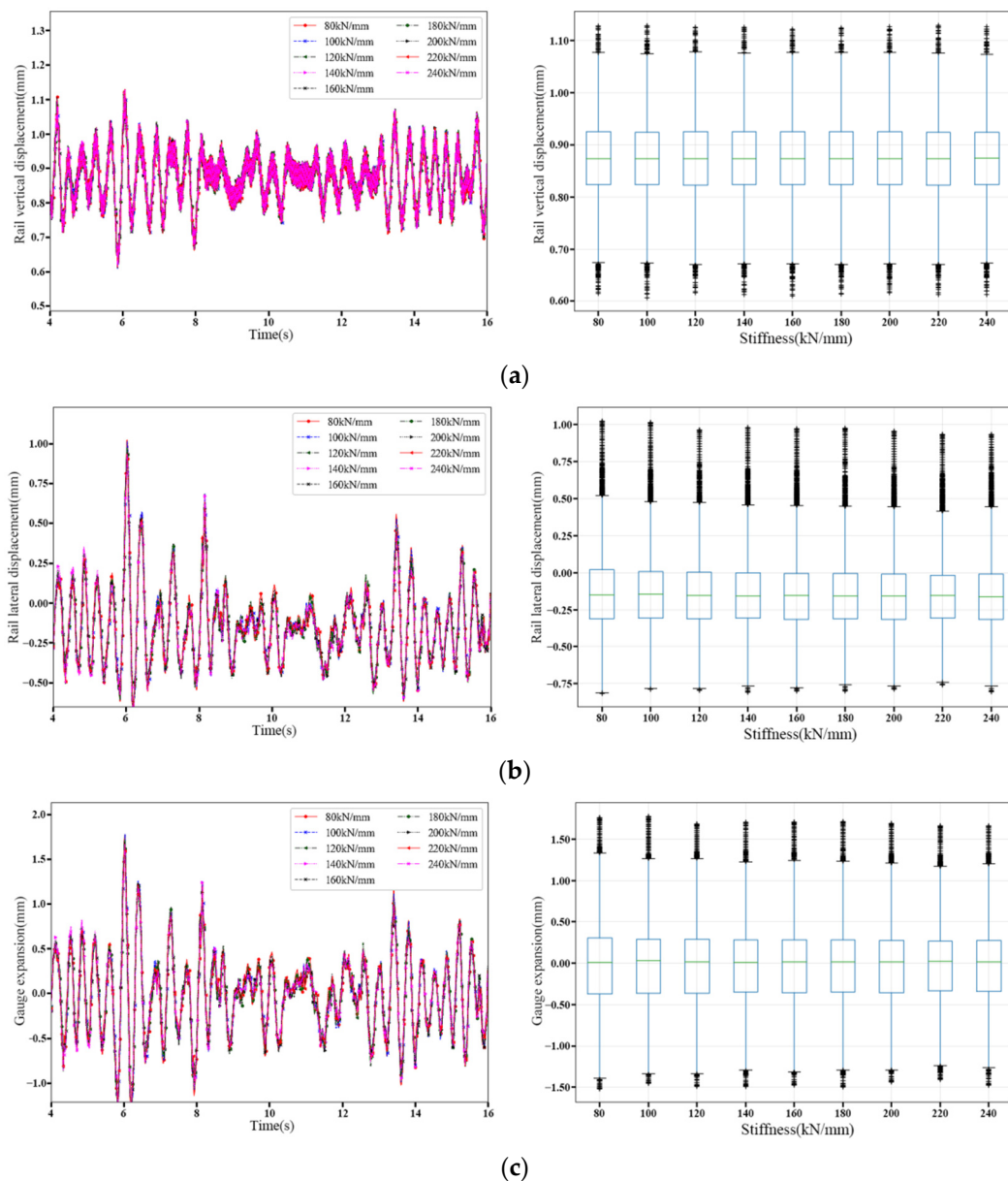


**Figure 13.** Variations in the deformation coefficients under different lateral stiffness under block. (a) Wheel-rail vertical displacement change: left-time history waveform, right-maximum, (b) Wheel-rail lateral displacement change: left-time history waveform, right-maximum and (c) Change in gauge expansion: left-time history curve, right-statistical distribution.

### 5. Analysis on Dynamic Response Sensitivity of Vehicle-Track System under the Change of Track Structure Parameters

#### 5.1. Analysis of the Trend of the Maximum Value of Each Index Changing with the Stiffness

Analysis of the trend of the maximum value of each index changing with the stiffness the maximum value of each index varies with stiffness, as shown in Figures 14–23, where the abscissas RB\_kz, RB\_ky, BB\_kz, BB\_ky in figures represent the vertical stiffness under rail, the lateral stiffness under rail, the vertical stiffness under block, and the lateral stiffness under block, respectively. Under the excitation of random track irregularities, the following results can be obtained by analyzing the variation tendency of each coefficient with each stiffness:

1. When the vertical support stiffness under rail increases, the vertical acceleration of the vehicle body does not change significantly with the increase in the vertical support stiffness under rail—the lateral acceleration of the vehicle body decreases first and

then increases, and the vertical displacement of the rail shows an exponential downward trend. The maximum values of other coefficients show a continuous fluctuation trend with the increase in vertical support stiffness under rail. The minimum values are 140 kN/mm and 200 kN/mm. Considering the changes in the various stability coefficient of the vehicle, it is more appropriate to set the stiffness of the vertical support under the rail to 120~160 kN/mm.

2. When the lateral support stiffness under rail increases, it can be seen that the vertical acceleration of the vehicle body does not change significantly with the increase in the stiffness of the lateral support under rail, and the lateral acceleration of the vehicle body varies greatly with the change of the support stiffness, and there is no obvious change feature. The wheel-rail vertical force and vertical displacement of rail are almost unchanged. The wheel-rail lateral force, the derailment coefficient and the wear coefficient show a trend of first decreasing and then increasing, and the wheel load reduction rate changes in the opposite way. Judging from the wheel-rail lateral force change curve, it is more reasonable when the stiffness of the lateral support block under the rail is in the range of 160~200 kN/mm.
3. When the vertical support stiffness under block increases, the vertical acceleration of vehicle body increases with the increase in the vertical support stiffness under block, the vertical displacement of the rail shows an exponential downward trend and the lateral acceleration of the vehicle body, wheel-rail lateral force, derailment coefficient, wheel load reduction rate, and wear coefficient follows a trend of first decreasing and then increasing, indicating that maintaining the vertical stiffness under block within a certain range can increase the lateral stability of the vehicle body. The wheel-rail vertical force changes little with the stiffness. Considering the change tendency of each driving safety coefficient comprehensively, the appropriate vertical stiffness under the block is 80~100 kN/mm.
4. When the lateral support stiffness under block increases, the vertical acceleration, the wheel-rail vertical force, lateral force, derailment coefficient, wheel load reduction rate, and wear coefficient do not change significantly. and the lateral acceleration of the vehicle body changes to a certain degree of volatility, but the amplitude is small near 220 kN/mm. Therefore, it is recommended that the lateral stiffness under the block should be within the range of 160~200 kN/mm.
5. Except for the vertical displacement of the rail, all the other indicators show a continuous fluctuation trend as the stiffness of the track structure changes. There are relatively large randomness and no obvious change characteristics. However, the ranges of change are small and all within the limits.

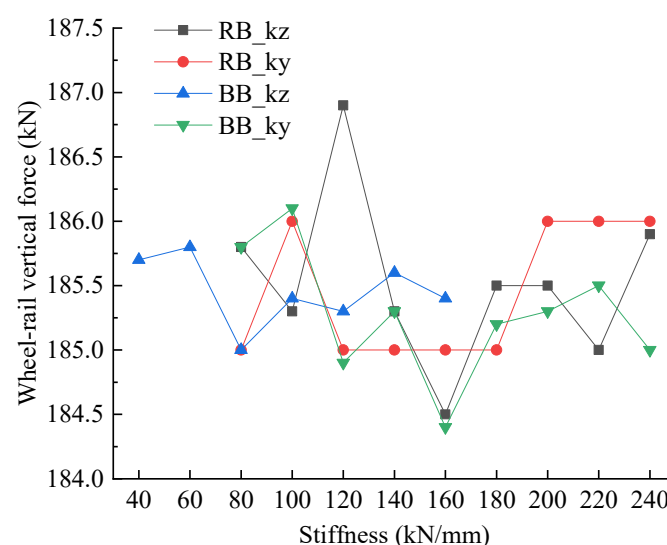


Figure 14. Variation trend of wheel-rail vertical force under different stiffness conditions.

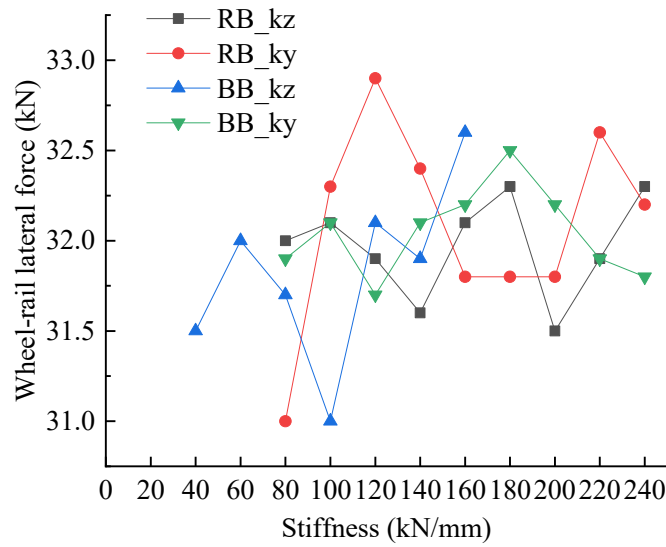


Figure 15. Variation trend of wheel-rail lateral force under different stiffness conditions.

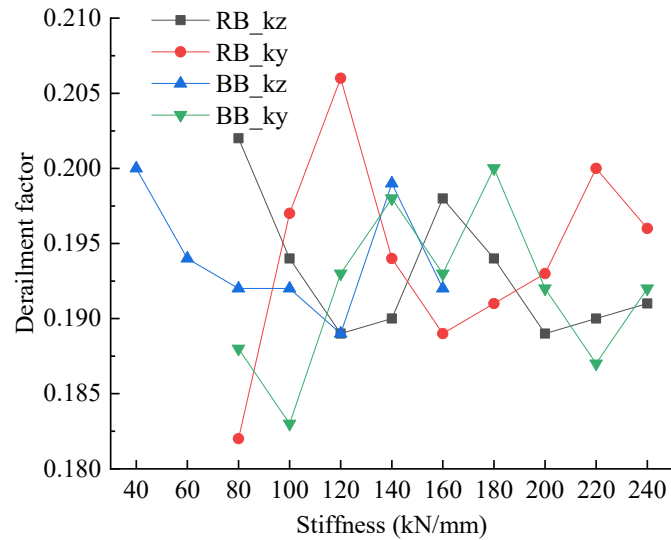


Figure 16. Variation trend of derailment coefficient under different stiffness conditions.

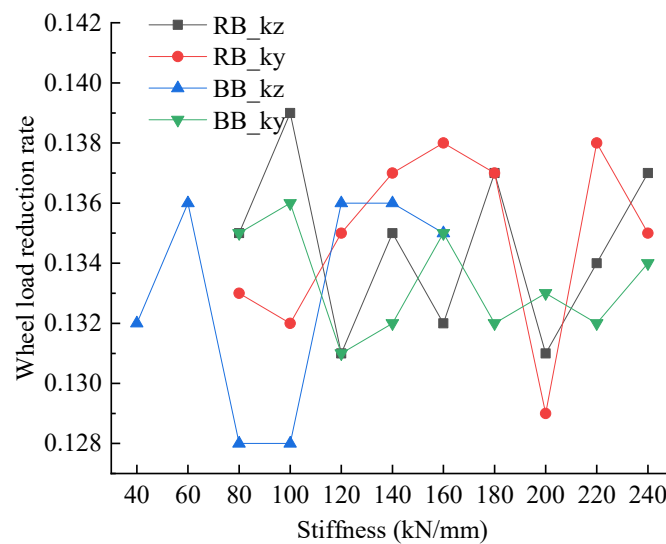


Figure 17. Variation trend of wheel load reduction rate under different stiffness conditions.

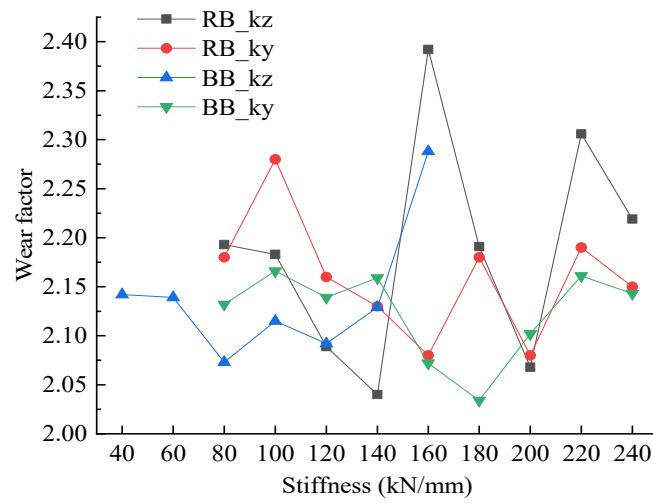


Figure 18. Variation trend of wear coefficient under different stiffness conditions.

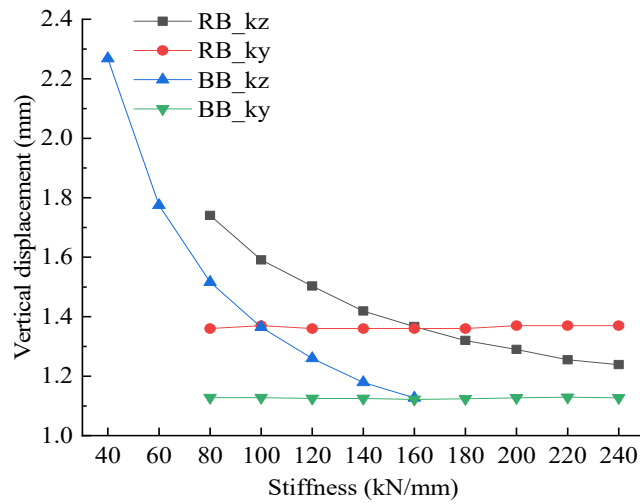


Figure 19. Variation trend of rail vertical displacement under different stiffness conditions.

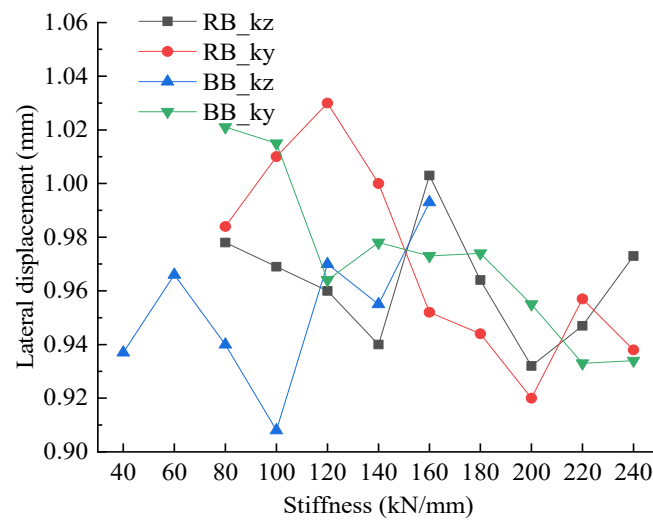


Figure 20. Variation trend of gauge expansion under different stiffness conditions.

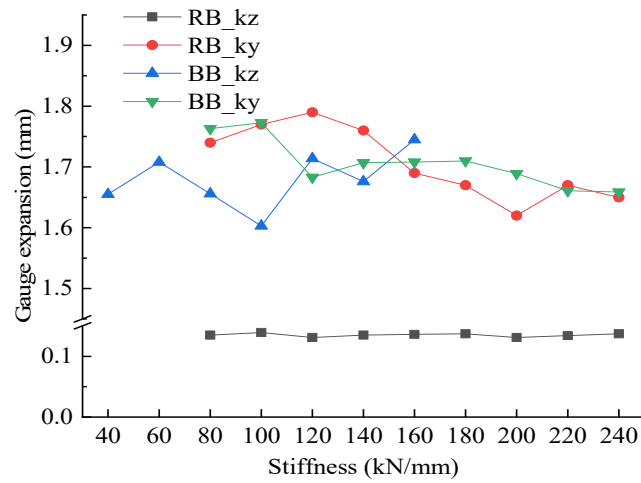


Figure 21. Variation trend of rail lateral displacement under different stiffness conditions.

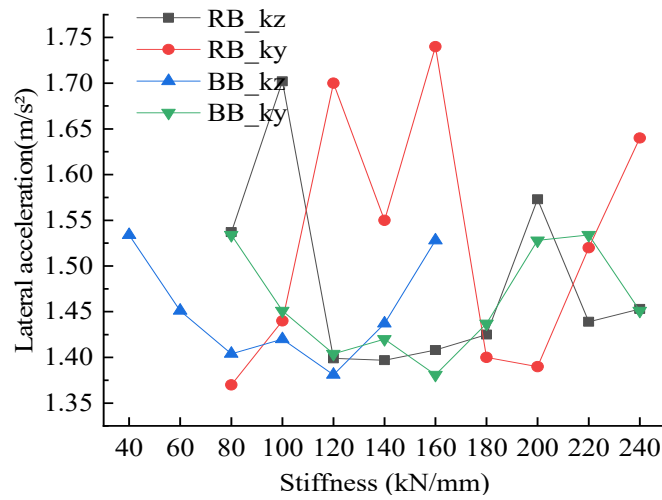


Figure 22. Variation trend of lateral acceleration of vehicle body under different stiffness conditions.

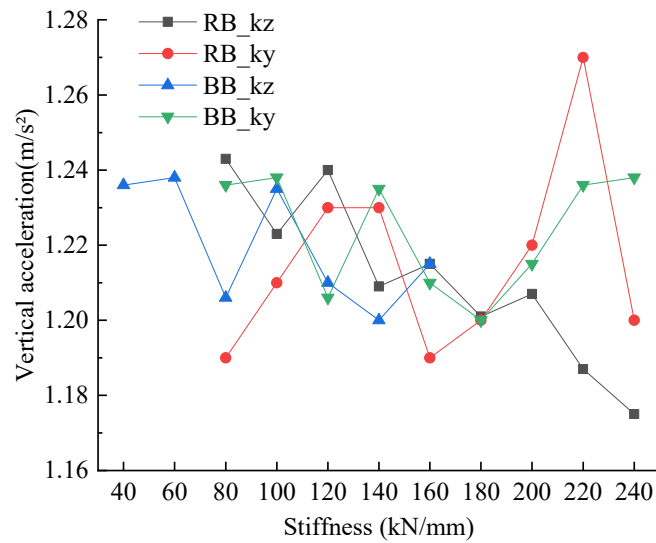


Figure 23. Variation trend of vertical acceleration of vehicle body under different stiffness conditions.

Note: The abscissas RB\_kz, RB\_ky, BB\_kz, BB\_ky in figures represent the vertical stiffness under rail, the lateral stiffness under rail, the vertical stiffness under block, and the lateral stiffness under block, respectively. The same is applied below.

### 5.2. Analysis of Sensitivity Indexes of Vehicle-Track System Dynamics Response

According to the research results of Sections 3 and 4, parts of the key dynamic performance of heavy-haul train and track structure system changes with track structure stiffness have been clearly analyzed to show the performance of the LVT under the action of a heavy-haul train. This section mainly studies the dynamic response sensitivity indexes of the vehicle-track system under different track structure parameter changes and discusses the degree of influence of different track structure parameters on the dynamic response of the vehicle-track system, which can provide a reference for the optimization design of LVT structure dynamics [27].

In order to accurately and quantitatively describe the changes in the dynamic response of the vehicle-track system, the ratio of the dynamic response change difference of the vehicle-track system to the stiffness change difference of the track structure is introduced as the sensitivity index of the dynamic response parameters, that is, the stiffness  $k$  of the track structure when it changes from  $k_1$  to  $k_2$ , will cause a certain dynamic response parameter  $D$  of the rail system to change from  $D_1$  to  $D_2$  [30], as shown in Equation (1):

$$\varepsilon_D = \frac{(D_2 - D_1)/(D_2 + D_1)}{(k_2 - k_1)/(k_2 + k_1)} \quad (1)$$

The world's main heavy-haul train countries and organizations, such as the United Kingdom, the United States, France, Germany, Japan, China and the International Union of Railways (UIC), etc., commonly used vehicle-track system dynamic response evaluation coefficients include wheel-rail lateral force, wheel-rail vertical force, wheel load reduction rate, wheel load reduction rate, wear coefficient, lateral acceleration of vehicle body, and lateral acceleration of vehicle body [26,31–38]. In addition, the reference [32] also puts forward the concept of track structure deformation coefficient, including vertical displacement of rail, lateral displacement of rail and gauge expansion. Therefore, this paper analyzes the sensitivity indexes of all the above evaluation coefficients to track structure parameters.

The sensitivity indexes of vertical stiffness under rail, lateral stiffness under rail, vertical stiffness under block, and lateral stiffness under block are, respectively, defined as  $\varepsilon_{iD}$  ( $i = 1\sim 4$ ). The dynamic response parameters of the rail system include wheel-rail vertical force, wheel-rail lateral force, derailment coefficient, wheel load reduction rate, wear coefficient, rail vertical displacement, rail lateral displacement, gauge expansion, lateral acceleration of vehicle body and vehicle acceleration of vehicle body. Its sensitivity indexes to the track structure parameters can be defined as  $\varepsilon_{iD,j}$  ( $i = 1\sim 4, j = 1\sim 10$ ).

In order to measure the degree of track structure parameters to the dynamic response of the vehicle-track system, the maximum response of the dynamic coefficient and the corresponding structural parameter value at this time are calculated. The sensitivity index can be expressed as shown in formula (2):

$$\varepsilon_D = \frac{(D_{\max} - D_{\min})/(D_{\max} + D_{\min})}{(k_2 - k_1)/(k_2 + k_1)} \quad (2)$$

The sensitivity index is the ratio of the rate of change of the dynamic response coefficient to the rate of change of the stiffness of the track structure. When  $k$  increases so that  $D$  increases, it is a positive value, otherwise it is a negative value. Table 8 summarizes the sensitivity indexes of vertical stiffness under different rails, lateral stiffness under rails, vertical stiffness under blocks, and lateral stiffness under blocks.

According to Table 12, it can be seen that there is different relationship between the dynamic response coefficient and the stiffness of the track structure:

1. When the vertical stiffness under rail changes, except for the vehicle body vertical acceleration sensitivity index which is positive, the other dynamic response parameter sensitivity indexes are all negative values, indicating that the vertical stiffness under rail increases, which is beneficial to reduce the rail system dynamic response level. In terms of the sensitivity to changes in the dynamic response parameters, the lateral acceleration of the vehicle body is the most obvious, while the vertical wheel-rail force, gauge expansion, and vertical acceleration of the vehicle body are not sensitive to changes in the vertical stiffness under rail, the wheel load shedding rate is the second, and the wear coefficient is, again, indicating that the vertical stiffness under rail is increased, which is beneficial to improve the dynamic stability of the vehicle body and reduce the wear between the wheel and the rail.
2. When the lateral stiffness under rail changes, the wear coefficient, the lateral displacement of the rail, the gauge expansion, and the lateral and vertical acceleration sensitivity indexes of the vehicle body are negative values, and the rest are positive values, indicating that the increase in the lateral stiffness under rail is beneficial to improve the lateral and vertical dynamic stability of rail system. In terms of the sensitivity of the changes in the dynamic response parameters of the rail system, the lateral acceleration of the vehicle body is the most obvious, followed by the vertical acceleration of the vehicle body, and the vertical displacement of the steel rail getting large, the wheel-rail vertical force and wheel load reduction rate are less affected by it.
3. When the vertical stiffness under block changes, except for the negative value of the wheel-rail vertical force and wheel load reduction rate, the sensitivity indexes of the other coefficients are all positive values, indicating that the increase in the vertical stiffness under block is not conducive to the overall rail system dynamic stability; in terms of sensitivity to changes in dynamic response parameters, the rail vertical displacement sensitivity is the highest, followed by the lateral acceleration of the vehicle body, and the wheel load reduction rate again, the vertical force of the wheel and rail, and the vertical acceleration of the vehicle body. The change of wheel-rail lateral force is less affected by the change of vertical stiffness under block, indicating that the dynamic response of the track system is highly sensitive to the influence of the vertical stiffness under block, and the vertical dynamic performance of the vehicle body is slightly affected by the vertical stiffness under block. The increase in vertical stiffness under block will intensify the lateral dynamic response level of the rail system.
4. When the lateral stiffness under block changes, the wheel-rail lateral force, wheel load reduction rate, and vehicle body lateral and vertical acceleration sensitivity indexes are positive values, and the other coefficients are negative values, indicating that the increase in lateral stiffness under block is beneficial to the track system. Improved dynamic performance will reduce the stability of train operation performance; in terms of sensitivity to changes in various dynamic response parameters, the lateral acceleration of the vehicle body is the most significant, followed by the vertical displacement of the rail, the gauge expansion again, and the sensitivity of other coefficients lower, indicating that although the increase in lateral stiffness under block is not conducive to the lateral dynamic stability of the vehicle body, it is conducive to maintaining the lateral stability of the track.

**Table 12.** Sensitivity indexes of vehicle-track system dynamic response under different track structure parameters.

Dynamic Response Coefficient of Vehicle-Track System	Track Structure Parameter Sensitivity Index			
	$\epsilon_{1D}$	$\epsilon_{2D}$	$\epsilon_{3D}$	$\epsilon_{4D}$
Wheel-rail vertical force	-0.018	0.044	-0.016	-0.020
Wheel-rail lateral force	-0.218	0.152	0.112	0.058
Derailement coefficient	-0.150	0.115	0.405	-0.185
Wheel load reduction rate	-0.337	0.047	-0.560	0.020
Wear coefficient	-0.332	-0.229	0.192	-0.097
Rail vertical displacement	-0.276	0.465	2.244	-0.357
Rail lateral displacement	-0.293	-0.191	0.184	-0.081
Gauge expansion	-0.083	-0.314	0.153	-0.211
Lateral acceleration of vehicle body	-0.404	-1.494	1.244	3.006
Vertical acceleration of vehicle body	0.031	-0.636	0.090	0.077

5.2.1. Wheel-Rail Contact Force Analysis

The change range of wheel-rail contact stress coefficient sensitivity indexes with different structural stiffness is shown in Figure 24, which shows:

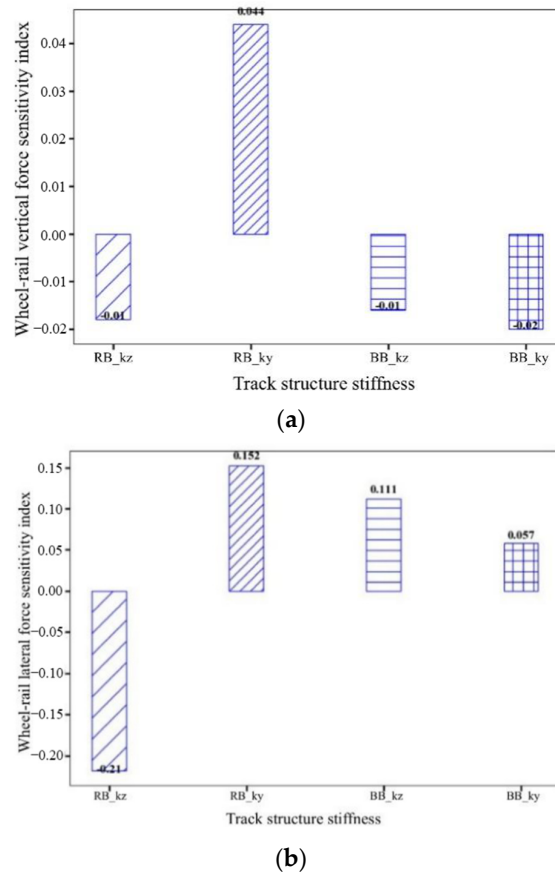


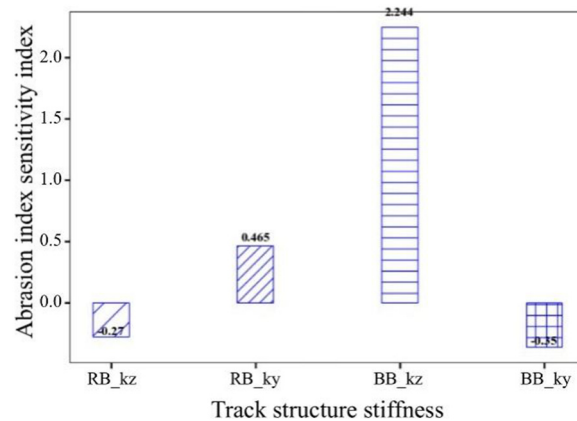
**Figure 24.** Sensitivity indexes of wheel-rail contact force coefficient. (a) Wheel-rail vertical force and (b) Wheel-rail lateral force.

The wheel-rail vertical force is less affected by the change of the track structure stiffness, and the wheel-rail lateral force is most affected by the vertical stiffness under rail but slightly affected by stiffness. Increasing the vertical stiffness under rail is beneficial to reduce the wheel-rail lateral force but increasing the lateral stiffness under rail will increase it, which is not conducive to maintaining the lateral train stability.

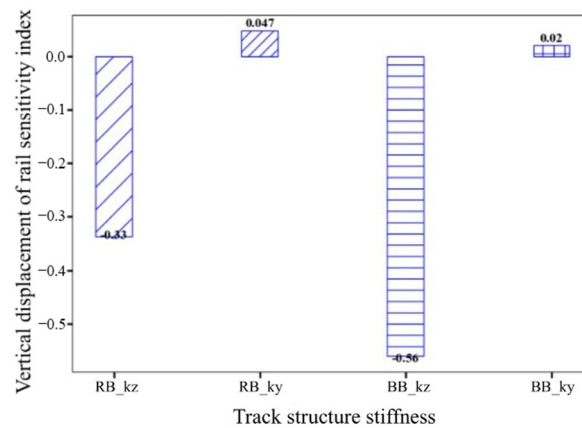
### 5.2.2. Vertical Ride Comfort Analysis

The change of vertical ride comfort coefficient sensitivity indexes with different structural stiffness is shown in Figure 25, which shows that:

1. The change tendency of the wear coefficient with the stiffness of the track structure are basically same. It is mostly affected by the vertical stiffness under block and increases with the increase in the vertical stiffness under block. Therefore, the larger the vertical stiffness under block, the higher the wear coefficient will be. It will adversely affect the service life of the rail, so the vertical stiffness under block should be set in a reasonable range to extend the rail change cycle;
2. The vertical displacement of the rail is significantly affected by the vertical stiffness of the track structure, while the lateral stiffness has little effect, and it is more affected by the vertical stiffness under block, which decreases with the increase in the vertical stiffness, indicating that a greater vertical stiffness under block is more conducive to maintaining the vertical smoothness of the track.



(a)

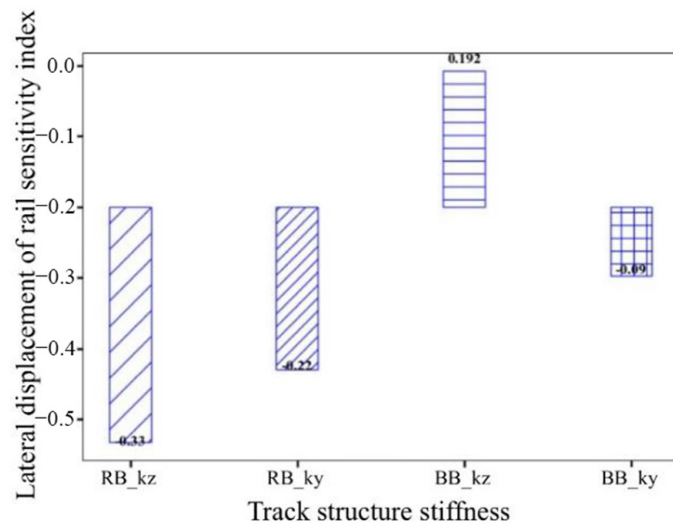


(b)

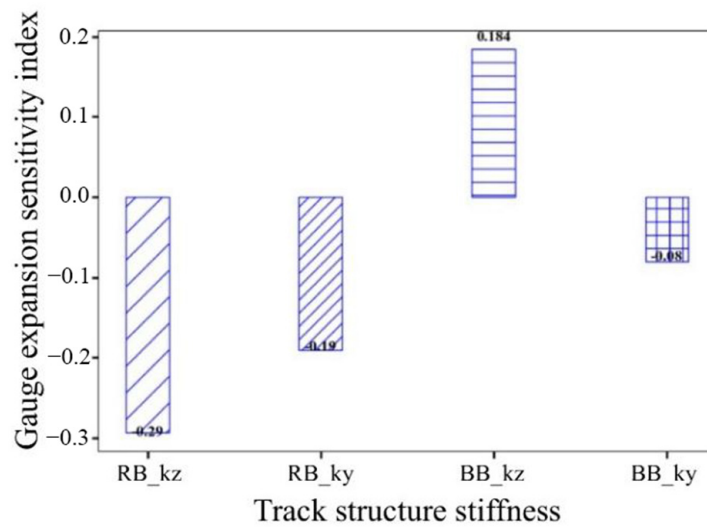
**Figure 25.** Vertical ride comfort coefficient sensitivity indexes. (a) Wear coefficient and (b) Vertical displacement of rail.

### 5.2.3. Lateral Ride Comfort Analysis

The change of the sensitivity indexes of lateral ride comfort coefficient with different structural stiffness is shown in Figure 26.



(a)



(b)

**Figure 26.** Lateral ride comfort coefficient sensitivity indexes. (a) Lateral displacement of rail and (b) Gauge expansion.

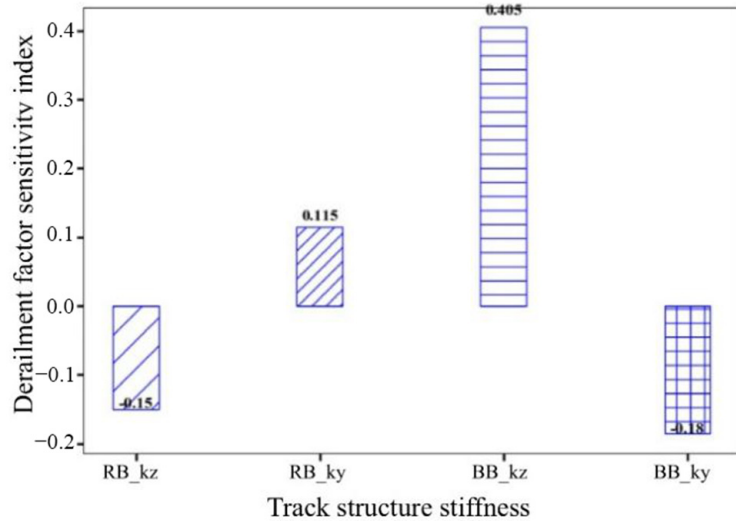
The rail lateral displacement and the gauge expansion are consistent with the change of the track structure and are most significantly affected by the vertical stiffness under rail. A larger vertical stiffness under rail can reduce the lateral displacement of the rail, thereby reducing the gauge expansion value, which is beneficial to guarantee the safety of train operation.

#### 5.2.4. Running Safety Analysis

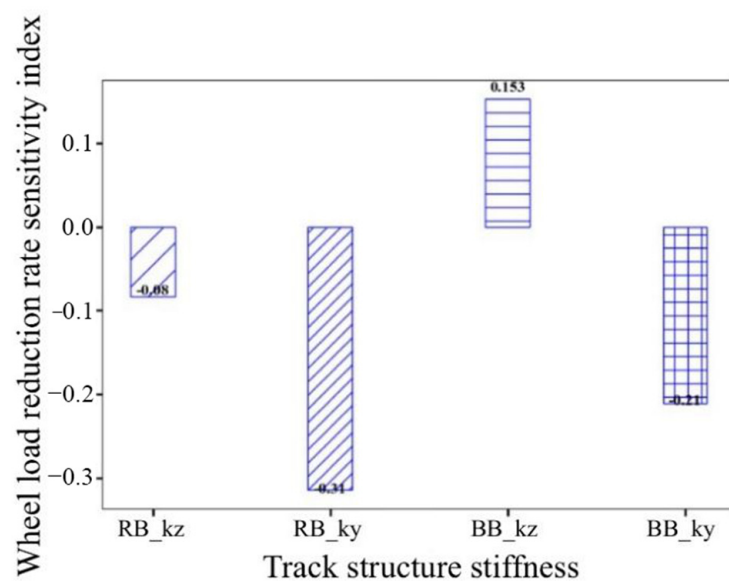
The change of the sensitivity indexes of running safety coefficient with different structural stiffness is shown in Figure 27, which shows that:

1. The derailment coefficient is most obviously affected by the change in the vertical stiffness under block and shows an increasing trend with the increase in the stiffness under block, and its value decreases when the other stiffness changes, indicating that the appropriate vertical stiffness under block is maintained and the remaining stiffness is appropriately increased. The stiffness of the track structure can reduce the risk of train derailment and ensure the safety of operation;

- The wheel load reduction rate is significantly affected by the under-rail and under-block lateral stiffness, and shows a decreasing trend as it increases, indicating that the larger lateral stiffness of the track structure can reduce the risk of train skipping.



(a)



(b)

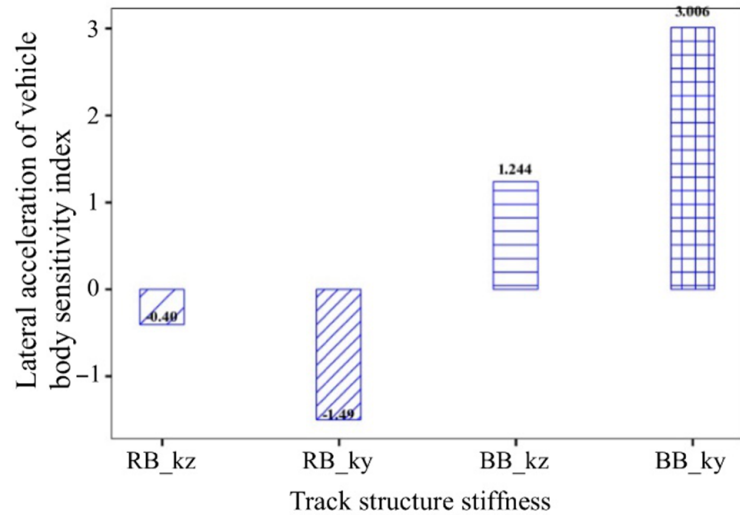
Figure 27. Sensitivity indexes of running safety coefficient. (a) Derailment coefficient and (b) Wheel load reduction rate.

### 5.2.5. Acceleration Analysis

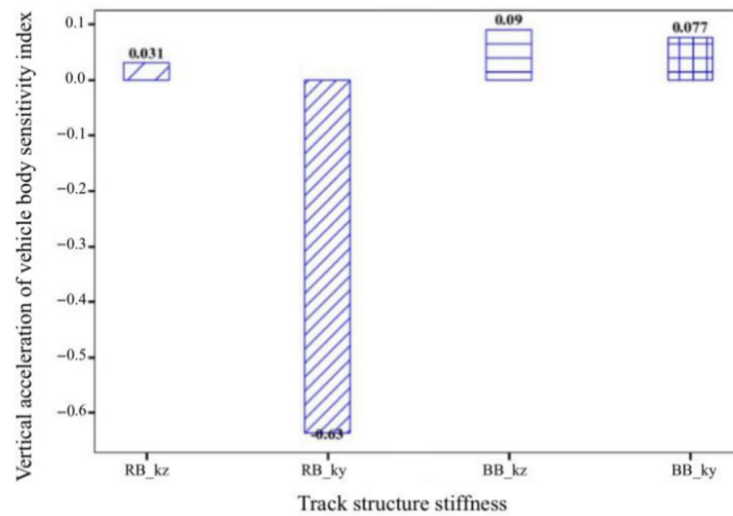
The change in curve of vehicle stability coefficient sensitivity indexes with different structural stiffness are shown in Figure 28, which shows:

- The lateral acceleration of the vehicle body is obviously affected by the change in the stiffness of the track structure. In particular, the increase in the lateral stiffness under block will cause the lateral acceleration of the vehicle body to increase significantly. In addition, it varies with the vertical stiffness under rail and the vertical stiffness under block. The lower lateral stiffness is the same, but the increase is small, and the change tendency of the lateral stiffness under rail is the opposite. Therefore, increasing the

- lateral stiffness under rail or reducing the lateral stiffness under block can improve the lateral train stability during operation;
- The vertical acceleration of the vehicle body is significantly affected by the lateral stiffness under rail, while the stiffness of the rest of the track structure has no obvious effect on it.



(a)



(b)

**Figure 28.** Sensitivity indexes of vehicle stability coefficient. (a) Lateral acceleration of vehicle body and (b) Vertical acceleration of vehicle body.

### 6. Conclusions

Based on the established coupled dynamics model of a heavy-haul train-LVT structure, this research investigated the influence of the under-rail and under-block stiffness changes on the dynamic performance of a heavy-haul train-LVT structure system, focusing on the sensitivity indexes of system dynamics response to explore the grading of the influence of different track structure parameters on the dynamic response of the vehicle-track system, providing a reference for the optimization design of LVT structure dynamics.

- When the rigidity of the vertical support under the rail increases, the lateral acceleration of the vehicle body decreases first and then increases, and the amplitude of the other stability coefficients fluctuates slightly and has a certain degree of randomness; the maximum value of the vertical displacement of the rail decreases, and the trend

gradually slows down, and the change tendency of the transverse displacement of the rail and the expansion of the gauge is not obvious. When the lateral stiffness under rail increases, the lateral acceleration of the vehicle body gradually increases, and the vertical acceleration of the vehicle body and the wheel-rail vertical force are basically unchanged. The wheel-rail lateral force and the derailment coefficient show a trend of first decreasing and then increasing, and the wheel load rate is opposite; the vertical displacement of the rail changes less, and the lateral displacement and gauge expansion decrease accordingly.

2. When the vertical support stiffness under block increases, the vehicle body vertical acceleration and wheel-rail vertical force change less, and the lateral acceleration of vehicle body, lateral force of wheel-rail, derailment coefficient and wheel load reduction rate show a trend of first decreasing and then increasing; The vertical displacement of rail gradually decreases, and the lateral displacement and gauge expansion show some randomness, but the overall trend is increasing. When the lateral stiffness under the block increases, the lateral acceleration of the vehicle body shows some volatility, and the remaining stability coefficients are basically unchanged; the vertical displacement of the rail has a small change, and the lateral displacement and the expansion of the gauge change simultaneously, and then show a decreasing trend.
3. An analysis of the sensitivity indexes change of the dynamic response coefficient of the integrated rail system showed that although the larger lateral and vertical structural stiffness under rail can reduce the dynamic response of the rail system, the vertical and lateral stiffness under block should be set within a reasonable range to achieve the purpose of reducing the dynamic response of the system. Additionally, beyond a certain range, the dynamic response of the vehicle-track system will increase significantly, which will affect the safety and stability of train operation.
4. In order to reduce the dynamic response of the rail system, the lateral and vertical stiffness under the rail should be increased as much as possible, but the vertical and lateral stiffness under the block should not be set in an excessively high range. Considering the change of track vehicle body stability coefficients, the change of deformation control coefficients and the sensitivity indexes of dynamic performance coefficients to track structure stiffness change; the recommended values of the vertical support stiffness under rail, the lateral support stiffness under rail, the vertical support stiffness under block, and the lateral support stiffness under block are, respectively 160 kN/mm, 200 kN/mm, 100 kN/mm, and 200 kN/mm.

**Author Contributions:** Conceptualization, Z.-P.Z. and W.-D.W.; methodology, Y.-C.X.; software, X.-G.D.; validation, J.-D.W. and Y.Y.; formal analysis, J.E.V.; investigation, Z.-L.X.; resources, L.-L.L.; data curation, X.-D.H.; writing—original draft preparation, Y.-C.X.; writing—review and editing, Z.-P.Z.; visualization, W.-D.W.; supervision, Z.-P.Z.; project administration, W.-D.W.; funding acquisition, Z.-P.Z. All authors have read and agreed to the published version of the manuscript.

**Funding:** The research is funded by the Open Fund Project of State Key Laboratory of High-speed Railway Track Technology, grant number 2021K002, High-Speed Railway Foundation Joint Fund Project, grant number U1734208; Natural Science Foundation of Hunan Province, China, grant number 2019JJ40384; Innovative experimental project for college students of Central South University, grant number 20210017020055.

**Institutional Review Board Statement:** Not applicable.

**Informed Consent Statement:** Not applicable.

**Data Availability Statement:** Experimental data has been presented in the context.

**Conflicts of Interest:** The authors declare no conflict of interest. The authors declare no potential conflicts of interest with respect to the research, authorship, and/or publication of this article.

## References

1. Zhai, W.; Gao, J.; Liu, P.; Wang, K. Reducing rail side wear on heavy-haul railway curves based on wheel–rail dynamic interaction. *Veh. Syst. Dyn.* **2014**, *52*, 440–454. [[CrossRef](#)]
2. Shi, J.; Burrow, M.P.N.; Chan, A.H.; Wang, Y.J. Measurements and simulation of the dynamic responses of a bridge–embankment transition zone below a heavy haul railway line. *Proc. Inst. Mech. Eng. Part F J. Rail Rapid Transit* **2013**, *227*, 254–268. [[CrossRef](#)]
3. Fen-Ling, F.; Dan, L. Heavy-haul train’s operating ratio, speed and intensity relationship for daqin railway based on cellular automata model. *Inf. Technol. J.* **2012**, *11*, 126–133. [[CrossRef](#)]
4. Wang, P.; Gao, L.; Hou, B.W. Influence of rail cant on wheel-rail contact relationship and dynamic performance in curves for heavy haul railway. *Appl. Mech. Mater.* **2013**, 365–366, 381–387.
5. Zhiwu, Y.; Zhi, S.; Ju, Y.; Xiao, L. Performance deterioration of heavy-haul railway bridges under fatigue loading monitored by a multisensor system. *J. Sens.* **2018**, *2018*, 5465391.
6. GonçalvesPereira, M.; Fernandes, L.; Leuschner, A.; Barreto, J.; Falcão, D.; Firmino, H.; Mateos, R.; Orrell, M. Development of a machine vision system for the inspection of heavy-haul railway turnout and track components. *Transp. Res. Rec. J. Transp. Res. Board* **2013**, *2376*, 71–80.
7. Bilow, D.N.; Randich, G.M. Slab Track for the Next 100 Years. In Proceedings of the Annual Conference Proceedings of American Railway Engineering and Maintenance of Way Association, Dallas, TX, USA, 10–13 September 2000.
8. Kucera, W.P.; Bilow, D.N.; Ball, C.G.; Li, D. Laboratory Test Results and Field Test Status of Heavy Axle Loads on Concrete Slab Track Designed for Shared High-Speed Passenger and Freight Rail Corridors. In Proceedings of the AREMA Annual Conference, Chicago, IL, USA, 5–8 October 2003.
9. Railway General Construction. No. 103, *Guiding Opinions on Optimization of Railway Engineering Design Measures*; China National Railway Group Co., Ltd.: Beijing, China, 2013.
10. Wu, B.; Li, S.; Zeng, Z.; Wang, W.; Wang, J.; Wu, Z. Static Load Test of Low Vibration Track under Heavy Haul Train. *J. Railw. Eng. Soc.* **2018**, *35*, 29–33. (In Chinese)
11. Zeng, Z.; Hu, G.; Wang, W.; Huang, X.; Wang, J. Research on the Mechanical Characteristics of Low Vibration Track. *Chin. J. Railw. Eng. Soc.* **2021**, *38*, 25–31. (In Chinese)
12. Zeng, Z.; Wang, J.; Yin, H.; Shen, S.; Shuaibu, A.; Wang, W. Experimental Investigation on the Vibration Reduction Characteristics of an Optimized Heavy-Haul Railway Low-Vibration Track. *Shock Vib.* **2019**, *2019*, 1539564. [[CrossRef](#)]
13. Zeng, Z.; Tian, C.; Chen, Z.; Wang, J.; Li, S.; Wu, Z. Test on impact vibration transmission and attenuation characteristics of low vibration track. *J. Traffic Transp. Eng.* **2020**, *20*, 82–92. (In Chinese)
14. Xu, G.; Su, S.; Wang, A.; Hu, R. Theoretical analysis and experimental research on multi-layer elastic damping track structure. *Adv. Mech. Eng.* **2021**, *13*, 168781402199497. [[CrossRef](#)]
15. Sung, D.; Chang, S.; Kim, S. Effect of additional anti-vibration sleeper track considering sleeper spacing and track support stiffness on reducing low-frequency vibrations. *Constr. Build. Mater.* **2020**, *263*, 120140. [[CrossRef](#)]
16. Piotrowski, J.; Kik, W. A simplified model of wheel/rail contact mechanics for non-Hertzian problems and its application in rail vehicle dynamic simulations. *Veh. Syst. Dyn.* **2008**, *46*, 27–48. [[CrossRef](#)]
17. Dettmar, J. *A Finite Element Implementation of Mooney-Rivlin’s Strain Energy Function in Abaqus*; University of Calgary: Calgary, AB, Canada, 2000.
18. Zhu, S.Y.; Cai, C.B. Interface damage and its effect on vibrations of slab track under temperature and vehicle dynamic loads. *Int. J. Non-Linear Mech.* **2014**, *58*, 222–232. [[CrossRef](#)]
19. Zhu, S.Y.; Luo, J.; Wang, M.Z.; Cai, C.B. Mechanical characteristic variation of ballastless track in highspeed railway: Effect of vehicle-track interaction and environment loads. *Railw. Eng. Sci.* **2020**, *28*, 408–423. [[CrossRef](#)]
20. Luo, J.; Zhu, S.Y.; Zhai, W.M. Development of a track dynamics model using Mindlin slab theory and its application to coupled vehicle-floating slab track systems. *Mech. Syst. Signal Process.* **2020**, *140*, 106641. [[CrossRef](#)]
21. Luo, J.; Zhu, S.Y.; Zhai, W.M. An advanced train-slab track spatially coupled dynamics model: Theoretical methodologies and numerical applications. *J. Sound Vib.* **2021**, *501*, 116059. [[CrossRef](#)]
22. Gong, C.; Feng, Q.; Sheng, X.; Lu, P.; Zhang, S. Using the 2.5D FE and transfer matrix methods to study ground vibration generated by two identical trains passing each other. *Soil Dyn. Earthq. Eng.* **2018**, *114*, 495–504.
23. Pogorelov, D.; Lei, Q.; Mikheev, G.; Rodikov, A. Development of dynamics simulation program for coupling vibration of maglev train-track beam based on UM. *Comput. Aided Eng.* **2019**, *28*, 28–35. (In Chinese)
24. Dou, H.; Wu, F.; Duan, Z.; Li, Z. Simulation Analysis of Longitudinal Impulse of Heavy-haul Train Based on UM. *J. Lanzhou Jiaotong Univ.* **2020**, *39*, 88–94. (In Chinese)
25. China Railway Fifth Survey and Design Institute Group Co., Ltd. *Research on the Optimization Design of Elastic Supporting Block Ballastless Tracks in Heavy-Haul Railway Tunnels*; Railway Fifth Survey and Design Institute Group Co., Ltd.: Beijing, China, 2017. (In Chinese)
26. *Chinese National Standards GB/T5599-1985. Railway Vehicles-S Pecification for Evaluation the Dynamic Performance and Accreditation Test*; National Bureau of Standards of China: Beijing, China, 1985. (In Chinese)
27. Liu, X. Effect analysis of track stiffness on dynamic characteristics of wheel-rail system and its dynamic optimization. *J. Southwest Jiaotong Univ.* **2004**, *1*, 1–5. (In Chinese)

28. Yang, C.; Li, F.; Fu, M.; Huang, Y. Research on the Matching Relationship between the Axle Load and Running Speed of Heavy Haul Freight Train. *China Railw. Sci.* **2012**, *33*, 92–97. (In Chinese)
29. Yang, C. Research on Matching Relationship between Axle Load & Running Speed of Heavy Haul Freight Wagon. Ph.D. Thesis, Southwest Jiaotong University, Chengdu, China, 16 August 2013. (In Chinese)
30. Zhang, G. Research on right level of track structure stiffness and track-part stiffness. *China Railw. Sci.* **2002**, *1*, 53–59. (In Chinese)
31. *Chinese National Standards TB/T2360-1993. Test Method and Evaluation Standard for Dynamic Performance Test of Railway Locomotive*; Ministry of Railways, PRC: Beijing, China, 1993. (In Chinese)
32. Zhai, W. *Vehicle-Track Coupling Dynamics*, 3rd ed.; Science Press: Beijing, China, 2015; pp. 213–225. (In Chinese)
33. Jia, L. Study on the Methods of Dynamic Performance Evaluation of High Speed Vehicles. Master's Thesis, Southwest Jiaotong University, Chengdu, China, May 2011. (In Chinese)
34. Zhai, W. Research on the Dynamics Performance Evaluation Standard for Freight Trains and the Suggested Schemes (1st Part Continued)—Evaluation Standard for Lateral Wheel-Rail Force. *Railw. Veh.* **2002**, *2*, 9-10+25-1.
35. Lv, K. Wheel-Rail Dynamic Evaluation Index for Spatial Alignment or High-Speed Railway. Master's Thesis, Southwest Jiaotong University, Chengdu, China, May 2016. (In Chinese)
36. Cai, C. Theory and Application of Vehicle-Track-Bridge Coupling Vibration in High-Speed Railways. Ph.D. Thesis, Southwest Jiaotong University, Chengdu, China, 19 November 2004. (In Chinese)
37. Ling, L. Study on the Dynamic Behaviour of High-Speed Train/Track Coupling System Composed of Multiple Vehicles. Master's Thesis, Southwest Jiaotong University, Chengdu, China, June 2012. (In Chinese)
38. Wan, J.; Wang, L. Simulation research on the dynamic characteristics of vehicle-track coupling system on the curved track of high-speed railway. *China Railw. Sci.* **2008**, *1*, 7–12. (In Chinese)